

PCA R&D Serial No. 2619

Properties of Self-Consolidating Concrete Containing Type F Fly Ash

by Raissa P. Douglas

NORTHWESTERN UNIVERSITY

**PROPERTIES OF SELF-CONSOLIDATING CONCRETE
CONTAINING TYPE F FLY ASH:**
WITH A VERIFICATION OF THE MINIMUM PASTE VOLUME METHOD

A THESIS
SUBMITTED TO THE GRADUATE SCHOOL
IN PARTIAL FULFILLMENT OF THE REQUIREMENTS

for the degree

MASTER OF SCIENCE
Field of Civil Engineering

By

RAISSA P. DOUGLAS

Evanston, Illinois

May 13, 2004

© Copyright by Raissa Patricia Douglas 2004
All Rights Reserved

Abstract

Since the introduction of self-consolidating concrete (SCC) in Japan during the late 1980's, acceptance and usage of this concrete in the construction industry has been steadily gaining momentum. In the United States, the usage of SCC has been spearheaded by the precast concrete industry. Good SCC must possess the following key fresh properties: filling ability, passing ability, and resistance to segregation. In order to reduce segregation, SCC mixes are typically designed with high powder contents, and contain chemical admixtures such as superplasticizers and viscosity modifying admixtures (VMA). This tends to increase the material cost of SCC, however one way to reduce the material cost is through adequate mix proportioning and the addition of supplementary cementitious materials such as fly ash. Millions of tons of fly ash are generated annually in Illinois; however Class F fly ash is more often landfilled than used. Incorporation of Class F fly ash in self-consolidating concrete as a means to replace portions of cement can decrease the cost of SCC, as well as further the sustainable development of concrete.

An experimental program, aimed at investigating the behavior of SCC containing Class F fly ash has been carried out. The fresh state properties of the concrete were assessed using methods of segregation and flow. The rheology of the paste matrix was also characterized and compared with a previously developed paste rheology model. Finally, some hardened state properties of the concrete were evaluated.

The objective of this research is to improve the understanding of the properties of SCC containing Class F fly ash and to provide information that could be used towards the commercialization of such a concrete. The results indicate that it is possible to develop a SCC containing Class F fly ash that is high performing in its fresh state. Furthermore, the addition of fly ash was shown to reduce superplasticizer dosage, increase workability, and increase overall chloride permeability resistance. In addition, it was determined that the difference of densities between the aggregate and matrix influence the results of a previously developed paste rheology model.

Acknowledgements

Pursuit of this degree has been a journey, but at the end I am much better for staying on this path. I thank the Lord for giving the strength to continue when I doubted myself and for all of his love and guidance. Secondly, I would like to thank my advisor, Professor Surendra Shah, for his patience, guidance, and encouragement. I would also like to thank the Dr. Van Bui for training me to be a “slump flow” expert and for the invaluable experience that I was able to pick up from being in his presence. I would also like to thank the Portland Cement Association (PCA) and Illinois Clean Coal Institute (ICCI) for funding this project.

I am also grateful to Dr. David Bonen and Dr. Yilmaz Akkaya for their advice and support. I would also like to thank Dr. Jeffrey Thomas, Dr. Bonen, and Professor Shah for participating in my defense committee. I would like to acknowledge the support of the Advanced Cement Based Materials Center staff, especially Steve Albertson and John Chiryal. I also would like to thank the post-docs, and visiting scholars at ACBM for all of their help.

I also gratefully acknowledge the support of fellow graduate students at Northwestern University especially, Katie Kuder, Zhihui Sun, Jay Terry, Laura Dykes, Lexyne McNealy, Deidra Morrison, Michele Manual, Ashley Smart, Ade Gordon, and Maisha Gray.

I am extremely grateful to Dean Penny Warren and the Office of Minority Affairs for being there whenever I needed anything. Thanks. I would also like to thank the Illinois Minority Graduate Incentive Program for directly funding me through out this degree.

I would like to thank my family for encouraging me, loving me, and being my rock at all times. Finally, I would like to thank my fiancée, Marcus Ferron, for not only being an excellent typist (smile), but also for being my #1 advocate.

ONWARDS TOWARD THE PhD!

Table of Contents

Abstract.....	i
Acknowledgements.....	ii
List of Figures.....	v
List of Tables.....	vii
Chapter 1 : Introduction	1
1.1 SCC: What is it?.....	1
1.2 Mix Proportioning.....	3
1.3 Fly Ash.....	4
1.4 Motivation.....	6
1.5 Objective and Scope	6
1.6 Organization.....	6
Chapter 2 :Fresh State Properties of Concrete.....	8
2.1. Introduction.....	8
2.2 Background.....	8
2.2.1 Fresh State Properties	9
2.2.1.a Filling Ability.....	9
2.2.1.b Passing Ability	10
2.2.1.c Stability	11
2.3 Testing Methods.....	12
2.3.1 Slump Flow Test.....	12
2.3.2 L-Box Test	14
2.3.3 Penetration Test	15
2.3.4 Experimental Program	16
2.3.4.a Materials.....	16
2.3.4.b Mix Proportions	18
2.3.4.c Mixing and Test Methods	18
2.4 Results and Discussion	19
2.5 Summary	21
Chapter 3: Fresh State Properties—Rheological Evaluation	22
3.1 Introduction.....	22
3.2 Background.....	22
3.2.1 Rheology.....	22
3.2.2 Rheological Models	26
3.2.2.a Self-Flow Zone Model.....	26
3.2.2.b Minimum Paste Volume Method.....	29
3.3 Experimental Program	34
3.3.1 Materials	34
3.3.2 Mixing Protocol	35
3.3.3 Flow test.....	36
3.3.4 Viscosity	36
3.4 Results and Discussion	36
3.4.1 Comparison with Rheological Model.....	36

3.4.1.a Paste Flow Diameter	37
3.4.1.b Apparent Viscosity.....	37
3.4.1.c Optimum Flow-Viscosity Ratio	38
3.4.1.d Effect of difference between densities of aggregates and paste	41
3.5 Summary	45
Chapter 4: Hardened Properties	47
4.1 Introduction.....	47
4.2 Background.....	47
4.2.1. Compressive Strength	47
4.2.2. Permeability	50
4.3 Testing Methods.....	56
4.3.1. ASTM C39 (Compressive Strength).....	56
4.3.2. RCPT.....	56
4.4 Results and Discussion	59
4.4.1. Compressive Strength	59
4.4.2. Permeability	61
4.5 Summary	66
Chapter 5 Conclusions.....	67
5.1. Introduction.....	67
5.2. Conclusions.....	67
5.3. Research Extensions	69
Appendix A: Sample Analysis to Determine Viscosity	74

List of Figures		pg
1.1	Timeline of SCC highlights	2
1.2	Schematic of SCC Fresh Properties	3
2.1	Excess Paste Theory	10
2.2	Stress generation due to relative displacement between aggregate	11
2.3	Schematic of upright and inverted slump test	13
2.4	Slump Flow of SCC	13
2.5	L Box with Penetration Apparatus	14
2.6	Flow through rebar in L-Box	15
2.7	Dimensions of L-Box	15
2.8	Penetration Apparatus	16
2.9	S45-F20 cross-section	20
2.10	Superplasticizer Dosage	21
3.1	Bingham model	23
3.2	Rheology testing methods	26
3.3	Spherical particle suspended in paste matrix	27
3.4	Self Flow Zone	29
3.5	Minimum paste volume theory	30
3.6	Minimum line for paste flow	32
3.7	Minimum line for viscosity	33
3.8	Model lines	33
3.9	Satisfactory zone obtained from combination of minimum flow diameter, minimum viscosity, and optimum flow/viscosity ratio	34
3.10	Paste flow diameter	35
3.11	Self flow zone	39
3.12	Viscosity comparison using combined approach and equilibrium approach	40
3.13	Paste flow and different products of $\Delta\rho$ and average radius (r_{av}) of aggregate	42

3.14	Viscosity and different products of $\Delta\rho$ and average radius (r_{av}) of aggregate	43
3.15	Paste flow-viscosity ratio and different products of $\Delta\rho$ and average radius (r_{av}) of aggregate	43
3.16	Relationship between flow/viscosity ratio and $P_{\Delta r}$	45
4.1	Compressive Strength Test Schematic	48
4.2	Range of typical strength to w/c ratio relationships of concrete based on over 100 different concrete mixtures	49
4.3	Compressive Strength Development of SCC with time in comparison with the regulations of Model Code 90	50
4.4	Relationship between total charge and initial current	54
4.5	RCPT Plot of 6 hr charge vs. 30 min charge	55
4.6	Initial current vs total charge for various researchers	55
4.7	Compressive Test Set up	56
4.8	RCPT Test Setup	58
4.9	Top View of RCPT Test Set up	58
4.10	Compressive Strength Results	61
4.11	Temperature profile	62
4.12	Initial current vs total charge	63
4.13	Extrapolated total charge vs. actual total charge	65
4.14	RCPT results	65

List of Tables pg

2.1	Fly ash composition	17
2.2	Coarse aggregate	17
2.3	Fine river sand	17
2.4	Concrete mix proportions	18
2.5	Overall fresh properties results	20
3.1	Rough estimate of typical SCC properties by countries	24
3.2	Paste mix proportions	35
3.3	Repeatability testing for viscosity	37
3.4	Paste flow diameter and viscosity	38
3.5	Product ($P_{\Delta r}$) of $\Delta\rho$ and r_{av}	42
4.1	Chloride ion penetrability test (RCPT)	52
4.2	Superplasticizer/binder	60
4.3	Chloride penetrability reduction percentages	66

Chapter 1 : Introduction

1.1 SCC: What is it?

Concrete, a composite material composed of cement, water, sand, and gravel, the world's most widely used construction materials. In 2003, more than 110 million metric tons of cement were consumed in the United States (U.S. Department of the Interior 2004), hence it is important to understand the properties of concrete in order to ensure safe and durable structures. When concrete is poured into the formwork it has a composition containing irregularly distributed pockets of entrapped air voids, and these air voids have an adverse effect on the surface appearance of concrete and the concrete properties. In order to eliminate the entrapped air and voids in concrete and to ensure proper bonding between the concrete and reinforcement, freshly placed concrete is consolidated. Consolidation is the process of inducing a closer arrangement of the solid particles in freshly mixed concrete by reduction of voids. During placement some consolidation is caused by gravity, but in order to ensure that concrete is properly consolidated additional methods are also employed. The most common method of consolidation is vibration (Mather and Ozyildirim 2002) and proper vibration of concrete ensures that the concrete is consolidated around the reinforcement and in the corners of the formwork. If the fresh concrete is allowed to harden without consolidation, then the resulting hardened concrete tends to be non-uniform, weak, porous, and poorly bonded to the reinforcement (Mather and Ozyildirim 2002).

To combat problems caused by improperly vibrated concrete, self-consolidating concrete (SCC) was developed at the University of Tokyo in Japan around 1988 by Professor Okamura and his students. Major highlights of the development of SCC is shown in Figure 1.1

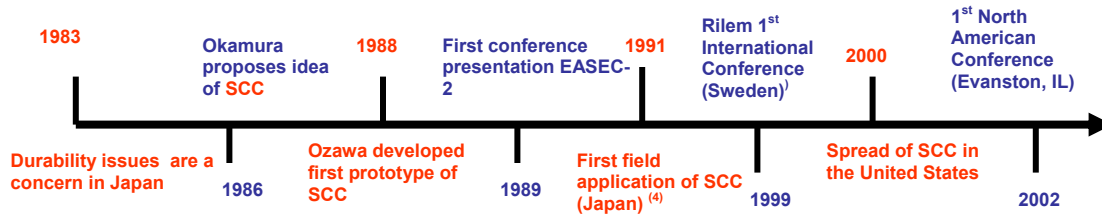


Figure 1.1: Timeline of SCC highlights

As its name implies, SCC is a concrete that is consolidated only through its self-weight, hence no additional compacting processes are needed. In addition, the composition of the concrete must remain uniform during placement and pumping. In order to be classified as an SCC the concrete must have the following key fresh properties: filling ability, passing ability, and resistance to segregation. Filling ability is the ability of the concrete to flow into and fill completely all spaces within the formwork under its own weight. Passing ability is the ability of the concrete to flow through tight openings (e.g. dense reinforcement) without any blocking. Resistance to segregation is the ability of the concrete to meet the filling ability and passing ability requirements while maintaining uniform composition (hence, no separation of aggregate from paste, or water from solids).

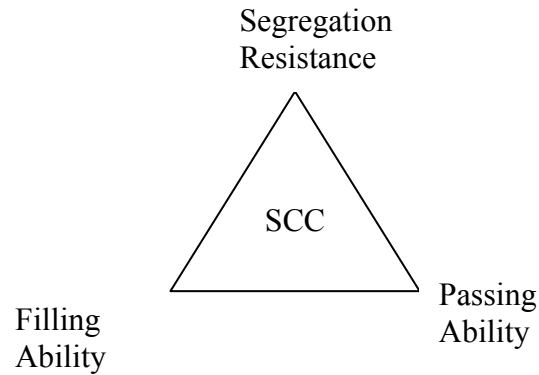


Figure 1.2: Schematic of SCC Fresh Properties

A major disadvantage of SCC is that there is a lack of globally agreed upon test standards and mix designs. Furthermore, SCC is normally created with a higher paste volume and chemical admixture content than normally vibrated concrete (NVC), and therefore the material cost of SCC often exceeds that of NVC. However, research and usage have shown that the usage of SCC technology reduces the total cost of labor, energy, required equipment and casting process. Therefore, when casting in highly congested areas, SCC is more productive, efficient, and has better constructability than conventional concrete.

1.2 Mix Proportioning

The development of SCC was basically conducted through trial and error, and to date there are no standard mix designs for SCC in the United States. However, it is commonly understood that in order to ensure flowability, yet at the same time maintain good segregation resistance, SCC should be designed with low yield stresses and adequate viscosities. Okamura et al. developed the first SCC by incorporating superplasticizer, optimizing aggregate grading and proportions, and including mineral admixtures such as

fly ash and silica fume (Okamura 1997; Bonen and Shah 2004). Today, segregation resistance is ensured by either incorporating large amount of fines or through the addition of viscosity-modifying admixtures (VMA). Hence, the rheological properties of SCC strongly depend on the methodology that is used to develop the SCC. NVC typically have yield stress values ranging from 500 to several thousands Pa, whereas SCC typically have yield stress values ranging 0 to 60 Pa. The viscosity of SCC mixtures range from 20 (incorporation of fines) to 200 Pa•s (incorporation of VMA) (Wallevik 2003).

The matrix phase is an important factor in determining the stability of SCC; hence, being able to predict the characteristics of SCC from the rheological properties of the matrix saves time, money, effort, and materials. Saak, Jennings, and Shah (2000) developed a methodology for designing SCC through its matrix phase by incorporating the concept of a “self-flow zone” and modeling the segregation resistance of one spherical particle suspended in the cement paste. In 2001, the model was expanded to include the effect of particle interaction (Bui, Akkaya et al.). The model was developed by testing a wide range concrete mixes with different coarse to total aggregate ratios (Nga), paste volume, cement content, fly ash content, and fly ash type. Although the model conducted tests on concrete mixes with different water to binder ratios (w/b), approximately 73% of those mixes had water to binder ratios of 0.38 – 0.40. In addition, only 12 of the concretes contained Type F fly ash.

1.3 Fly Ash

Fly ash is the finely divided residue resulting from the combustion of coal. It is a pozzolanic material that is commonly used in cement-based materials and the particles are generally finer than cement particles. A pozzolan is a material that provides a source of silica to combine with the calcium hydroxide in concrete to form a calcium silica hydrate (C-S-H)

product that is similar to the C-S-H product formed during the hydration of portland cement. The primary reaction is depicted in equation 1.1.



Fly ash is approximately half the price of cement, and in addition to its economical benefits, the use of fly ash in has been reduces permeability, bleeding, water demand and the heat of hydration. It also improves workability, however strength development is slower. For every ton of cement that is a manufactured, approximately one ton of carbon dioxide gas, the main green house gas, is released into the environment. From an environmental perspective, one of the benefits of fly ash is that the replacement of large portions of cement with fly ash serves to reduce CO₂ emissions, thus making concrete an even greener material that it already is. However, not all fly ash is suitable for concrete, and because the chemical composition of fly ash widely varies ASTM C 618 provides a classification system based on its coal source. Class C fly ashes are produced from the burning of lignitic or subbituminous coals and are primarily found in western states. Class F fly ashes are produced from the burning of bituminous and anthracite coals and are primarily found in states east of the Mississippi River (Mindess, Young et al. 2003). The most common coals found in the Illinois region are high volatile bituminous coals (Illinois State Geological Survey 2003), however, Class C fly ash is more often used in construction by the Illinois Department of Transportation. Class F fly ash have a higher carbon content and lower calcium oxide (lime) content than Class C fly ash, and only exhibits pozzolanic properties when it is introduced to water. However, due to its high calcium oxide content, Class C fly ash exhibits pozzolanic and cementitious properties when introduced to water.

1.4 Motivation

The usage of SCC is rapidly growing in the United States, however, there is a need to decrease the material cost, develop globally agreed upon test methods, and a gain a deeper understanding of SCC technology. One way to reduce the material cost of SCC is through adequate mix proportioning and the addition of supplementary powder materials, such as fly ash. However, the properties of fly ash greatly depend on the region in which it is obtained, and therefore, the properties of SCC containing Illinois fly ash should be evaluated in order to determine if it is possible to produce a good quality SCC with fly ash from the Illinois region. The results of this project should provide information that will help reduce the material cost of SCC, further sustainable development in the concrete industry, and contribute to the development and usage of SCC in the United States and the global community.

1.5 Objective and Scope

The objective of this project was to investigate the fresh properties of SCC containing Illinois Class F fly ash. In addition, the permeability and compressive strength were also evaluated. The rheological properties of the cement paste were evaluated and compared with the results from a previously developed paste rheological model.

1.6 Organization

Chapter 2 reviews the key fresh state properties of SCC and discusses common testing methods. In addition, the results on the fresh performance of the concrete are presented. Chapter 3 presents a review of rheology and the rheological models used to analyze the cement paste. The results from the rheological program are also discussed. In Chapter 4, hardened state properties are discussed and testing procedures used to evaluate compressive

strength and chloride permeability are presented. The results and analysis of the hardened state properties of the concrete is also discussed. Chapter 5 contains a summary of the experimental findings and lists the important conclusions that were drawn throughout the study. This chapter also provides suggestions for areas in which future work is warranted.

Chapter 2 :Fresh State Properties of Concrete

2.1. Introduction

In this chapter, a discussion of the fresh properties and the empirical testing methods used to evaluate these properties is given. In addition, an experimental program was conducted to evaluate the fresh state properties and the results of that study are presented.

2.2 Background

Self-consolidating mixes are designed to have fresh properties that have a higher degree of workability than NVC. Workability is a way of describing the performance of concrete in the plastic state and for SCC, workability is often characterized by the following properties: filling ability, passing ability, and stability (segregation resistance) (PCI FAST Team 2003). A concrete can be characterized as an SCC only if all three of these properties exist. Like NVC, workability requirements for SCC will differ depending on the application, and it is imperative that these properties are maintained at an adequate level during the transport and placement. Through adequate mix proportioning the attributes of passing ability, stability, and filling ability can be obtained at a reasonable price. Similar to NVC, there are no specific mix proportions defining SCC mixes, and the mix compositions and proportions of SCC vary depending on the concrete engineer, job conditions, and available materials.

Many tests (Ferraris 1999) have been developed in order to measure the workability of concrete mixes, but most of these tests are empirically based and are not able to characterize the three major properties in a single test. Although these tests were developed to assess concrete workability, they are often method specific and do not give the basic material properties. In the United States there are no standard test methods to evaluate the fresh state properties of SCC, but organizations such as the American Concrete Institute

(ACI), American Society of Testing and Materials, International Union of Laboratories and Experts in Construction Materials, Systems, and Structures (RILEM), and many others, are working on specifications and standards for SCC construction. A guide discussing common field problems in manufacturing and construction of SCC and ways to prevent them was published by The Japan Society of Civil Engineers (Ouchi and Nakajima 2001). In 2002, the European Federation of Producers and Contractors of Specialist Products for Structures (EFNARC) created the “Specification and Guidelines for Self-Compacting Concrete” in order to provide a framework for design and use of SCC (EFNARC). And recently, the Prestressed Concrete Institute (PCI) published the “Interim Guidelines for the Use of Self-Consolidating Concrete in PCI Member Plants” as a provisional guide for precast producers until comprehensive standards are developed (PCI FAST Team 2003).

2.2.1 Fresh State Properties

2.2.1.a Filling Ability

Filling ability, or flowability, is the ability of the concrete to completely flow (horizontally and vertically upwards if necessary) and fill all spaces in the formwork without the addition of any external compaction. The flowability of SCC is characterized by the concrete’s fluidity and cohesion, and is often assessed using the slump flow test (details about this test are given in section 2.3.1). In 1940, C.T. Kennedy proposed the “Excess Paste Theory” as a way to explain the mechanism governing the workability of concrete. This theory states that there must be a enough paste to cover the surface area of the aggregates in order to attain workability, and that the excess paste serves to minimize the friction among the aggregates and give better flowability. Without the paste layer, too much friction would be generated as the aggregates moved and workability would be impossible. In 2003, Nielsson and Wallerik designed SCC with decreased filling ability by only altering the paste composition while keeping the aggregate composition

the same, and confirmed the theory that filling ability is primarily a function of the cement paste matrix. Although the primary reason for the development of SCC was to combat durability issues, its high flowability also can reduce the cost of labor and accelerate construction schedules.

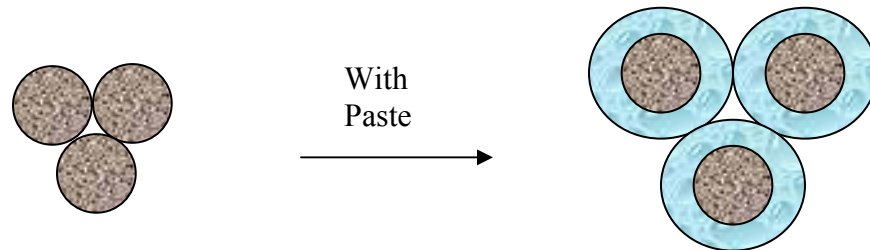


Figure 2.1: Excess Paste Theory

2.2.1.b Passing Ability

Passing ability is the ability of the concrete to flow through restricted spaces without blocking. This property is related to the maximum aggregate size and aggregate volume, and the L-Box test is the most common method used to assess this property. A visualization experiment conducted by Dr. Hashimoto (Okamura 1997) showed that blockage occurred from the contact among coarse aggregates. As the distance between particles decreases, the potential for blocking increases due to particle collisions and the build-up in internal stresses. Inter-particle interaction can be reduced by decreasing the coarse aggregate volume, and it has been shown that the energy required to initiate flow is often consumed by the increased internal stresses and coarse aggregates. Therefore, Okamura recommends that the aggregate content should be reduced in order to avoid blockage (Okamura and Ouchi 1999).

As concrete approaches and flows through narrow spaces, a difference occurs in the velocities of the aggregate and the relative location of the aggregate changes. This velocity difference results in the matrix preceding the aggregates through the space and hence the aggregate content is locally increased as new aggregate particles flow into the area and add to the

remaining particles (Noguchi, Oh et al. 1999). The relative displacement from the change in aggregate location causes shear stress in addition to compressive stresses, and in order for the concrete to flow smoothly through the narrow spaces the shear stress should be minimized (Okamura and Ouchi 1999).

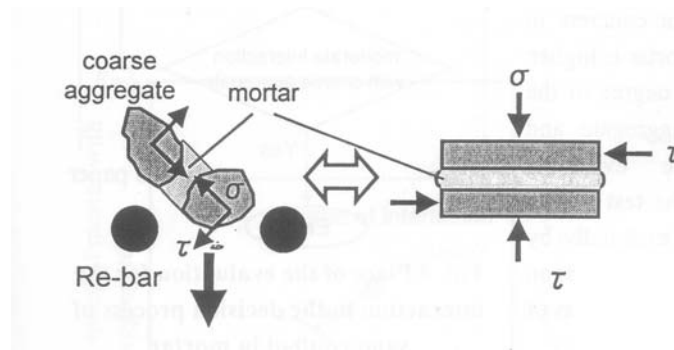


Figure 2.2: Stress generation due to relative displacement between aggregate (Okamura and Ouchi 1999)

As a result, the viscosity of the paste should be high enough to prevent the localized increases in the internal stress due to the coarse aggregate particles approaching each other (Okamura and Ouchi 1999). Segregation resistance is largely controlled by viscosity, and if the aggregates segregate then this could lead to blockage, therefore the viscosity of the paste should also be high enough to prevent segregation that may occur due to the increased aggregate content

2.2.1.c Stability

Stability, or resistance to segregation, is the ability of the concrete to remain uniform and cohesive throughout the entire construction process (mixing, transporting, handling, placing, casting, and etcetera). There should be minimum segregation of the aggregates (both fine and coarse) from the matrix and little bleeding. Bleeding is a special case of segregation in which

water moves upwards and separates from the mix. Some bleeding is normal for concrete, but excessive bleeding can lead to a decrease in strength, high porosity, and poor durability particularly at the surface. Stability is largely dependent on the cohesiveness and viscosity of the concrete mixture, and cohesiveness and viscosity can be increased by reducing the free water content and increasing the amount of fines. A reduction of free water content has been shown to improve stability while decreasing inter-particle friction among solid particles (Khayat and Monty 1999). In order to ensure adequate stability, there are two basic mixture-proportioning methods: using a low water/cement ratio (w/c) and high content of fines, or by incorporating a viscosity-modifying admixture (VMA) (Bonen and Shah 2004). The former approach is based on the Japanese method and incorporates the use of a superplasticizer (SP), low water/cement, high powder content, mineral admixtures, and low aggregate content, whereas the latter approach uses a low or moderate powder content, SP and VMA.

2.3 Testing Methods

2.3.1 Slump Flow Test

The Slump-Flow test is the most commonly used test for evaluating SCC. This inexpensive test is a modified version of slump test (ASTM C143), and it was originally developed in Japan to test underwater concrete. The testing apparatus consists of a mold in the shape of a frustum of a cone with a base diameter of 8 inches, a top diameter of 4 inches, and a height of 12 inches and a rigid plate. The mold is placed on top of the plate and is filled with concrete. Next, the mold is lifted vertically upwards and the horizontal spread of the sample is measured in two perpendicular directions after the concrete stops flowing. In addition, the time that it takes the concrete to reach a diameter of 50 cm (T_{50}) is also recorded as an indicator of the concrete flowability. A modified version of this test is often performed by inverting the slump cone. When the slump test is performed with the cone upright, the

cone has a tendency to float up while the cone is being filled. The extra pressure needed to prevent the cone from lifting restricts the movement of the person filling the cone and hence two people are often used to conduct the test—one person to fill the cone and another person to hold the cone stationary. Correlation studies have shown that there is no difference in slump flow and T_{50} results when the inverted cone method is used instead of the upright cone method (Ramsburg 2003).

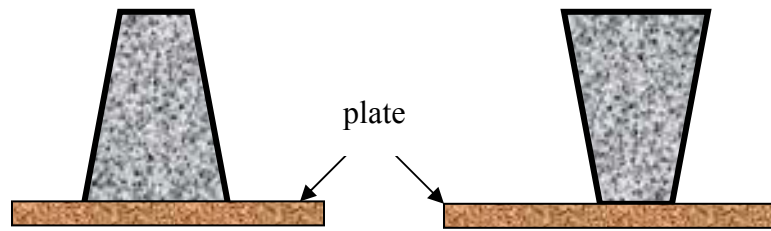


Figure 2.3: Schematic of upright and inverted slump test

It has been stated that the segregation tendency of the concrete can also be determined from visual observation of the spread (EFNARC 2002). Although the slump flow test is used as an indication of fluidity, filling ability can not be sufficiently evaluated by using the slump test alone, and other tests like the L-Box test should be used too.



Figure 2.4: Slump Flow of SCC

2.3.2 L-Box Test

The L-box test was also developed in Japan to test underwater concrete, and it has been adopted to test highly flowable concretes. This test consists of an L-shaped box in which the vertical and horizontal ends are separated by a sliding door (Figure 2.5). Concrete is poured into the vertical leg, and the sliding door is raised to allow the concrete to flow into the horizontal section. Typically, reinforcement bars are placed at the entrance of the horizontal section to gauge the passing ability of the concrete (Figure 2.6). Generally, the spacing of the reinforcing bars should be three times the maximum aggregate size (Ferraris 1999). After the concrete stops flowing, the height of the concrete left in the vertical section (h_1) and at the end of the horizontal section (h_2) are measured. The ratio of h_2/h_1 is an indication of the passing ability of the concrete. Although there is no standardized dimensions for the L-box, those listed in Figure 2.7 seems to be the most common (Bui, Montgomery et al. 2002).



Figure 2.5: L Box with Penetration Apparatus



Figure 2.6: Flow through rebar in L-Box

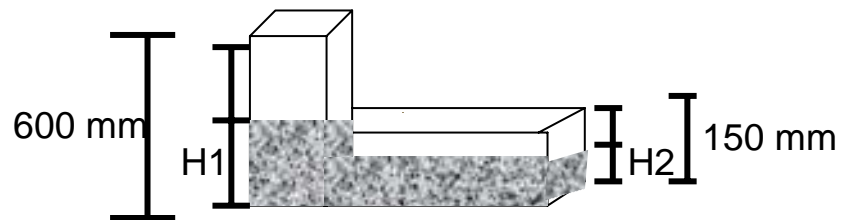


Figure 2.7: Dimensions of L-Box

2.3.3 Penetration Test

A testing method and apparatus to determine the segregation resistance of concrete in both the horizontal and vertical direction was developed in 2002 by Bui, Montgomery, and Turner (Bui, Montgomery et al. 2002). The apparatus is used in conjunction with the L-Box (Figure), and consists of a hollow cylindrical penetration head that is assembled from a hollow cylindrical mold and a rod (Figure 2.8). The entire mass of the penetration head is 54g with an inner diameter, height, and wall thickness of 75 mm, 50 mm, and 1 mm, respectively. The bottom part of the rod is attached to the hollow cylindrical mold and the upper part slides through a slot in the frame. A reading scale (ruler) is attached to the frame for measuring the depth that the penetration apparatus sinks into the concrete. This depth is called the penetration depth (P_d).

Two minutes after pouring concrete into the L-Box and prior to opening the gate, the apparatus is placed on top of the vertical leg of the L-box. The apparatus is adjusted until the penetration cylinder is just touching the surface of the concrete and then the cylinder is allowed to sink freely into the concrete. After 45 seconds the P_d is recorded. Concrete with a P_d greater than 8mm is considered to have poor segregation resistance.

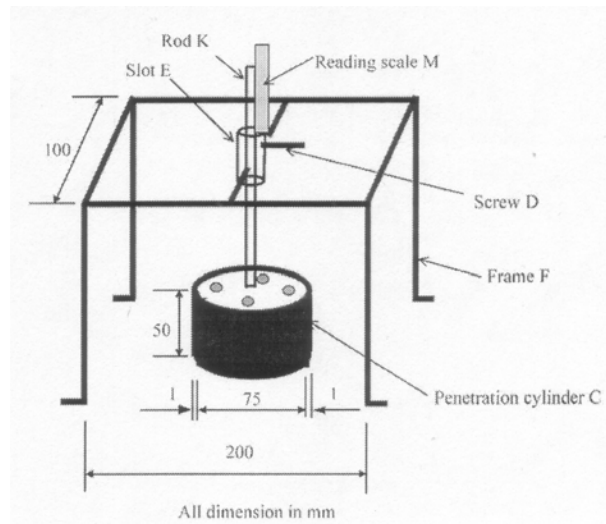


Figure 2.8 Penetration Apparatus (Bui, Montgomery et al. 2002)

2.3.4 Experimental Program

2.3.4.a Materials

Ordinary (Type 1) Portland Cement (OPC) and Vermillion (Type F) Fly Ash were used. The physical and chemical properties of the fly ash are listed in Table 2.1. Fine river sand and 19mm diameter gravel were used as the aggregates. The physical properties and particle size distributions are provide in Tables 2.2 and 2.3. A polycarboxylate-based superplasticizer (Axim Catexol-Superfluc 2000 PC) was used.

Table 2.1: Fly ash composition

Property	Class F Fly Ash
Silicon Oxide (SiO ₂), %	47.47
Aluminum Oxide (Al ₂ O ₃), %	26.36
Ferric Oxide (Fe ₂ O ₂), %	12.16
Calcium Oxide (CaO), %	5.40
Sulfur Trioxide (SO ₃), %	1.06
Magnesium Oxide (MgO), %	0.90
Loss on Ignition (LOI), %	2.17
Specific Gravity	2.27
Fineness (+325 Mesh), %	15.90
Moisture Content, %	0.05
Soundness, %	-0.02
S.A.I, 7 days , %	85.80

Table 2.2: Coarse Aggregate

Screen Size (mm)	% Passing
19	100
15.625	100
12.5	84
9.5	43
4.75	3
0	0
Specific gravity	2.62
Absorption (%)	1.3

Table 2.3: Fine river sand

Screen Size (mm)	% Passing
9.5	100
4.75	99
2.36	83
1.18	63
0.6	41
0.3	15
0.15	4
0.075	1.9
0	0
Specific gravity	2.69
Absorption (%)	2.3

2.3.4.b Mix Proportions

A total of six concrete mixes were tested. The proportions of the concrete mixes are summarized in Table 2.4. The mixes were prepared by varying the water/binder ratio (w/b) while keeping the paste volume constant and gravel/total aggregate ratio (Nga) constant. W/b ratios of 0.35 and 0.45 were used. The paste volume for all mixes was 364L/m³ with an Nga = 0.52. Fly ash replacement was conducted on a mass basis. Fly ash replacements of 0%, 20%, and 30% were tested.

Table 2.4: Concrete Mix Proportions

Mix	Constituent						
	<i>Gravel</i> (kg/m ³)	<i>Sand</i> (kg/m ³)	<i>Cement</i> (kg/m ³)	<i>Fly Ash</i> (kg/m ³)	<i>Water</i> (kg/m ³)	<i>SP</i> (kg/m ³)	<i>W/B</i>
S35-F0	884	816	516	0	179	2.18	0.35
S35-F20	882	814	399	100	175	1.57	0.35
S35-F30	881	814	344	147	172	1.25	0.35
S45-F0	882	814	449	0	202	0.94	0.45
S45-F20	882	814	349	87	196	0.9	0.45
S45-F30	882	814	301	123	194	0.91	0.45

2.3.4.c Mixing and Test Methods

All mixes were prepared by mixing aggregates (fine and coarse), fly ash, and cement for one minute. Then the mixing water was added, and the batch was mixed again for one minute. After waiting 30 seconds, the batch was mixed for two minutes, and then the superplasticizer was added and the batch was mixed for an additional two minutes. The inverted slump-flow test

was conducted and the T_{50} and the final diameter of the concrete after it stopped flowing were recorded (see Figure 2.4). Next, the penetration test and the L-box test were conducted. The concrete's mold surface quality was observed after concrete filled into the vertical portion of the L-Box, which was made of plexi-glass. Then the passing ability test with an L-box was undertaken, and the H2/H1 ratio was calculated (higher H2/H1 ratio indicates greater passing ability of SCC). The concrete was also poured into 100 x 200mm cylindrical plastic molds and covered with a plastic sheet in order to prevent water evaporation. The cylinders were demolded after one day and placed in a curing room at 100% relative humidity until the compressive strength tests and permeability tests were performed.

2.4 Results and Discussion

Overall data for the fresh concrete properties are presented in Table 2.5 and Figure 2.10. It is commonly accepted that a $T_{50} < 12s$, concrete flow diameter (F_d) $> 600mm$, and $H2/H1 \geq 0.8$, will produce a good performing SCC (Bui, Montgomery et al. 2002). The slump flow of all mixtures ranged from approximately 650mm to 750mm, and this indicates good deformability. All mixes had similar slump flow times (average 3 seconds). All mixes had good flowability, and addition of fly ash content did not affect the slump flow time. As indicated by the H2/H1 ratio, all mixtures exhibited good passing ability and no blockage was exhibited in any of the mixes. Previous research has shown that a penetration depth greater than 8 mm is an indication that an SCC would be prone to high segregation (Bui, Montgomery et al. 2002). All mixes displayed good resistance to segregation, and good mold-surface finish ability, except mix S45-F0, which had a little honeycombing in the cast cylinders. Since the penetration depth of S35-F20 was 8 mm, a check for

segregation was conducted. Figure 2.9 shows a cross section of the hardened concrete and there appears to be no segregation of the coarse aggregates.



Figure 2.9: S45-F20 cross-section

Table 2.5: Overall fresh properties results

Mix	T50 (s)	(F _d) (mm)	P _d (mm)	H2/H1
S35-F0	3.5	749	4	0.87
S35-F20	4	690	5	0.80
S35-F30	3	657	3	0.75
S45-F0	3	708	1	0.79
S45-F20	3	724	8	0.75
S45-F30	2	750	3	0.75

As seen in Figure 2.10, for a given w/b, addition of fly ash generally results in a reduction of superplasticizer for a similar workability (flow diameter). Furthermore, as expected, for similar workability, increasing the water/binder ratio reduces the amount of superplasticizer required. Lastly, at

the higher w/b, superplasticizer requirement is less sensitive to the addition of addition of fly ash.

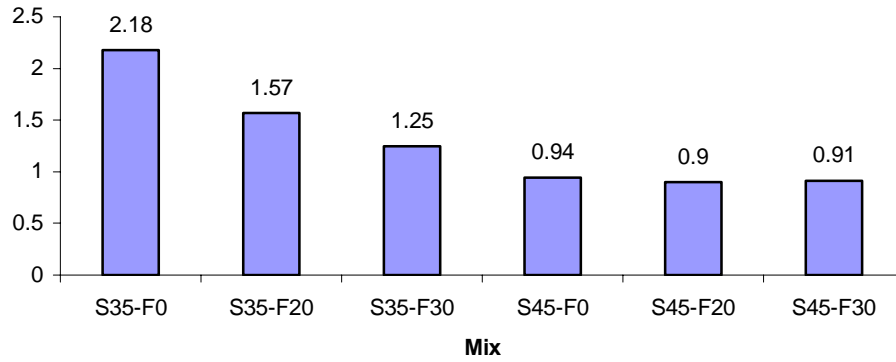


Figure 2.10: Superplasticizer Dosage

2.5 Summary

A high performance SCC mixture containing Type F fly ash from the Illinois region was produced. The slump flow test, penetration test for segregation, and L-box test were undertaken to investigate the fresh properties of the concrete. All mixtures exhibited satisfactory flowability, segregation resistance, and passing ability of SCC. Addition of fly ash generally resulted in a reduction of superplasticizer for a similar workability.

In Chapter 3, the fresh state properties of the paste will be evaluated.

Chapter 3: Fresh State Properties—Rheological Evaluation

3.1 Introduction

In the previous chapter, the fresh state properties of concrete were qualitatively assessed using empirical methods and a good performing SCC was produced. In this chapter, these same properties will be evaluated using a rheological approach. A review of the rheological aspect of cementitious materials is presented. In addition, a previously developed paste rheological model is discussed, and the results from the rheological model are compared with the performance of the concrete developed in Chapter 2.

3.2 Background

3.2.1 Rheology

Rheology is the study of the deformation and flow of matter under stress (Tattersall and Banfill 1983), and knowing the rheological parameters (yield stress and viscosity) of a fluid provides a quantitative and fundamental way of characterizing the filling ability and stability of SCC. For a Newtonian fluid the shear stress is directly proportional to the shear rate and the material properties are described by the constant of proportionality. This is the simplest form of flow behavior and mathematically it is expressed as $\tau = \eta\dot{\gamma}$, where τ is the shear stress, η is the viscosity and $\dot{\gamma}$ is the shear rate. Immediately, it follows that the viscosity is the constant of proportionality that represents the characteristic behavior of the material. Unfortunately, cementitious materials are more complicated, and they can not be described by a single constant. At low shear rates, fresh concrete flow behavior follows the Bingham model and mathematically this relationship is represented as, $\tau = \tau_0 + \mu\dot{\gamma}$, where τ_0 is the yield stress and μ is the plastic viscosity.

The yield stress is the shear strength of the material. This is the strength that must be exceeded in order for flow to begin. In a plot of shear

rate vs. shear stress, the yield stress is the point at which the slope of the line crosses the ordinate axis (Figure 3.1). Once the yield stress is exceeded the material flows and the viscosity (η) is the material resistance to flow. For a Bingham fluid, the relationship between viscosity and plastic viscosity is $\eta = \mu + \frac{\tau_0}{\dot{\gamma}}$. Hence, the plastic viscosity is the viscosity limit at high shear rates.

Bingham Model: $\tau = \tau_0 + \mu \dot{\gamma}$

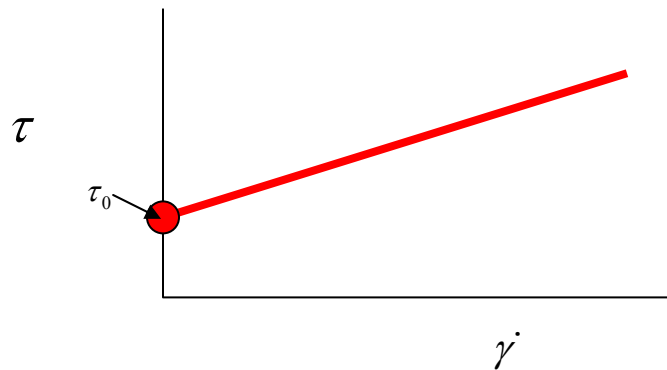


Figure 3.1 Bingham model

Yield stress values for NVC range from 500 Pa to a several thousands Pa, but SCC are designed with low yield stresses varying from zero to 60 Pa (Table 3.1). Similarly, the viscosity of SCC also varies from 20 Pa•s to over 100 Pa•s (Wallevik 2003). A low yield stress and viscosity is needed for SCC in order to impart high fluidity and retain kinetic energy (Bonnen and Shah 2004).

Table 3.1: Rough estimate of typical SCC properties by countries (Nielsson and Wallevik 2003)

	Powder (kg/m ³)	Water (kg/m ³)	Yield value (Pa)	Pl. viscosity (Pa s)
Sweden	>550	180	0-30	50-100
The Netherlands	>550	190	0-10	60-120
Japan	>550	170	0-30	50-120
France	?	?	0-10	>60
Switzerland	<450	200	0-50	10-20
Norway	<450	170	10-50	30-45
Iceland	<450	180	10-50	20-40
Denmark	<400	160	30-60	<40
UK	>500	210	10-50	50-80
Germany	>500	180	0-10	60-90
US	>500	190	0-20	40-120

In regards to stability, a high yield stress counteracts sedimentation and a high plastic viscosity reduces the rate of sedimentation. Since the yield stress of SCC is not large enough to counteract sedimentation, the viscosity of the paste largely controls the rate of sedimentation. Hence a balance must be achieved in which the paste viscosity is high, but the overall viscosity of the concrete is designed to be as low as possible. Generally, partial replacement by mass of cement with fly ash has been shown to reduce the yield stress and viscosity of cement paste and concrete. Studies have shown that for a given particle distribution, water demand is decreased at the highest packing density (Ferraris, Karthik et al. 2001). Spherical particles have been shown to achieve higher packing densities than crushed particles (Sakai, Hoshimo et al. 1997). Therefore, it has been hypothesized that the increase in workability is a result of a reduction in water demand and a decrease in interparticle friction due to the spherical shape of fly ash particles (Ferraris, Karthik et al. 2001).

Concrete is a thixotropic material, meaning that the apparent viscosity decreases in time with increasing shear rate. This decrease in viscosity is a due to preferentially orientation of the particles which results in the shear stress increasing less rapidly than the shear rate. Hence, it is easier to increase the flow rate of the material. A hysteresis loop is typical of a thixotropic material,

and a truly thixotropic material exhibits fully reversible behavior. A typical hysteresis loop for concrete is shown in Figure 3.2 (a). The exact shape of the hysteresis loop depends on the properties of the substance, the shape of the flow curve, and shear stress axis intercept. The hysteresis loop method provides a direct way of measuring viscosity, yield stress, and structural breakdown. A disadvantage of using the hysteresis loop testing method is that the entire structural breakdown of the material may not be captured since the loop captures a range between the peak and equilibrium stress for a given shear rate. An alternative method for capturing the entire flow behavior of concrete is the equilibrium method (Figure 3.2 (b)). This method studies the rate of structural breakdown with time at a constant shear rate. The difference between the peak and equilibrium stress is a measure of the material's thixotropy. The major disadvantage of the equilibrium method is that multiple samples must be tested in order to obtain the flow curve. In 2000, Saak developed an approach in which the both the peak and equilibrium stress curves of cement paste could be obtained from one sample. This approach combines the hysteresis loop and equilibrium methods into one testing program and is shown schematically in Figure 3.2(c). In this program, the shear rate is ramped from 0s^{-1} to a maximum value, then the shear rate is held at the maximum value for a set amount of time, and finally the shear rate is ramped down from the maximum value to 0s^{-1} .

Understanding the rheology of SCC is important because not only can it be used as a tool to accurately describe the workability of SCC, but it can also aid in the design of future SCC mixes.

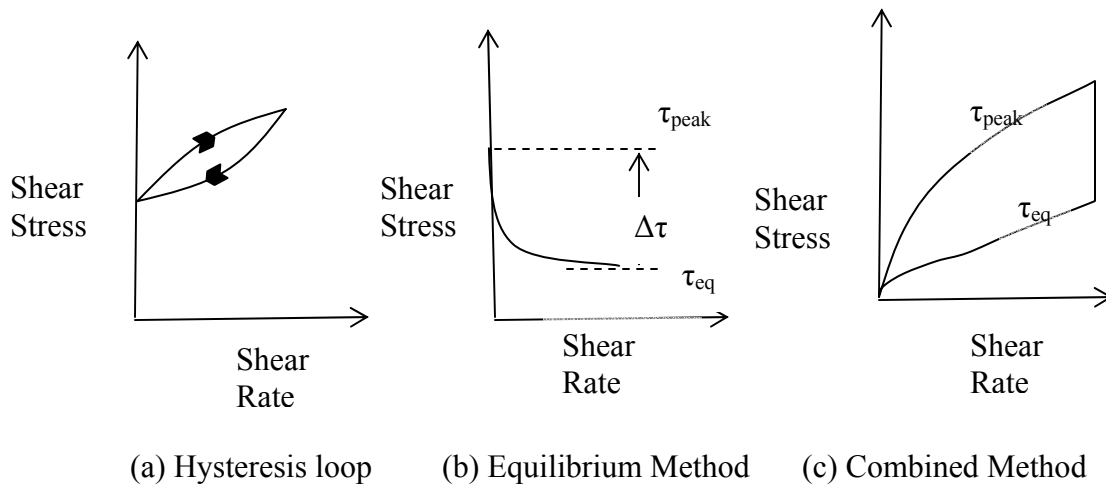


Figure 3.2: Rheology testing methods

3.2.2 Rheological Models

3.2.2.a Self-Flow Zone Model

A design methodology for SCC was proposed by Saak, Jennings, and Shah (Saak, Jennings et al. 2001), and this model is based on the assumption that a minimum yield stress and viscosity is needed in order to prevent segregation. The model was derived for the quasi-static case of a single particle suspended in a cementitious matrix. By balancing the forces acting on a single spherical particle, a criterion was developed for estimating the minimum yield stress and viscosity necessary to prevent segregation. A brief derivation of the model will be given.

Consider the case of a spherical aggregate suspended in a cementitious matrix as shown in Figure 3.3:

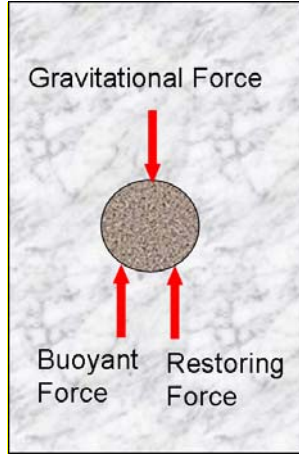


Figure 3.3: Spherical particle suspended in paste matrix

The resulting downwards force acting on the particle is the difference between the gravitational force and the buoyant force.

$$F_{down} = F_{grav} - F_{buoy} \quad \text{Equation 3.1}$$

The gravitational force (F_{grav}) and the buoyant force (F_{buoy}) are given as:

$$F_{grav} = g\rho_a V_{agg} \quad \text{Equation 3.2}$$

$$F_{buoy} = g\rho_m V_p \quad \text{Equation 3.3}$$

where g is the gravitational constant, ρ_a is density of the aggregate, V_{agg} is the volume of the aggregate, and ρ_m is the density of the matrix. Therefore,

$$F_{down} = g\Delta\rho V_{agg} \quad \text{Equation 3.4}$$

where $\Delta\rho$ is the density difference between the aggregate and the matrix is

$$\Delta\rho = \rho_a - \rho_m \quad \text{Equation 3.5}$$

Using principles of equilibrium, it is easy to see that the restoring force (F_{res}) must be at least equal to the F_{down} in order to prevent segregation. The restoring force is given as:

$$F_{res} = \tau_y A_{agg} \quad \text{Equation 3.6}$$

where τ_y is the yield stress of the matrix. For a spherical particle, if

$$\tau_y < \frac{4}{3} g \Delta \rho r_a \quad \text{Equation 3.7}$$

then segregation will occur, where r_a is the radius of aggregate. Under dynamic conditions, the restoring force is replaced by the drag force (F_{drag}) which is given as:

$$F_{drag} = C_D \rho_m \frac{v^2}{2} A_{agg} \quad \text{Equation 3.8}$$

where C_D is the drag coefficient and v is the terminal falling velocity of the

$$\text{particle. By force balance, } v = \sqrt{\left(\frac{4}{3}\right) \left(\frac{g \Delta \rho r_a}{C_D \rho_m}\right)}. \quad \text{Equation 3.9}$$

The drag coefficient is inversely related to Reynolds number (R_e), and for a

$$\text{sphere } R_e = \frac{2r_p \rho_m v}{\eta}. \quad \text{Equation 3.10}$$

$$\text{Therefore, } C_D \propto \frac{1}{R_e} \propto \frac{\eta}{\rho_m}. \quad \text{Equation 3.11}$$

In order to minimize segregation, the terminal falling velocity should be minimized. From the relationship between the drag coefficient and Reynolds number, it is apparent that this condition requires a high matrix viscosity. It is also apparent that segregation resistance is a function of the viscosity and the yield stress of the paste. Furthermore, both the viscosity and yield stress of the paste are functions of the density difference between the aggregate and the matrix and the size of the particle. Hence, for a given aggregate particle size distribution, there is a minimum viscosity and yield stress needed to prevent segregation. This concept led to the development of

the “self-flow zone” theory. The underlying principle of this theory is that there is a minimum viscosity at which the concrete is able to flow without segregating and there is a maximum viscosity at which the concrete is able to maintain good segregation resistance and still be highly flowable. If the yield stress or viscosity is too high, the concrete will have low workability, and if the yield stress or viscosity is too low the concrete will segregate (Figure 3.4).

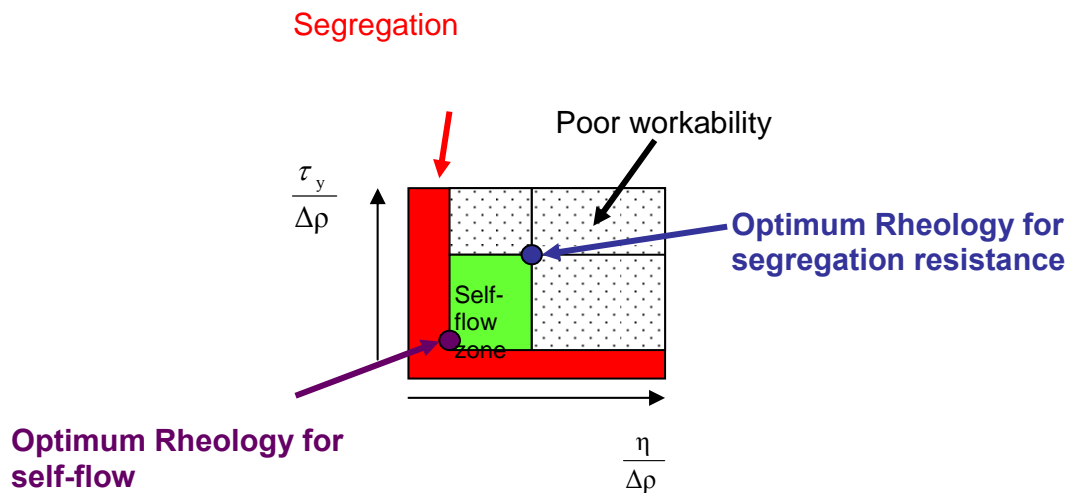


Figure 3.4 Self Flow Zone

3.2.2.b Minimum Paste Volume Method

The self-flow zone theory was developed for a single particle suspended in cement paste. A rheological model for self-consolidating concrete was developed by Bui, Akkaya, and Shah (Bui, Akkaya et al.) and this model is an expansion of the self-flow zone model and it takes into account aggregate particle interaction. Similar to the Excess Paste Matrix theory (Kennedy 1940), the underlying concept of this model is that a minimum paste volume is necessary to completely coat the aggregates and fill any voids in order to ensure good deformability. If the paste volume is too

small, the concrete will have poor flowability. It is commonly believed that the rheology of the paste governs the segregation resistance, passing ability, and filling ability of the resulting SCC concrete. It has been shown that segregation resistance is affected by aggregate diameter. Hence the average aggregate diameter (D_{av}) and average aggregate spacing (D_{ss}) were used as parameters to account for aggregate influence in the model (Figure 3.5).

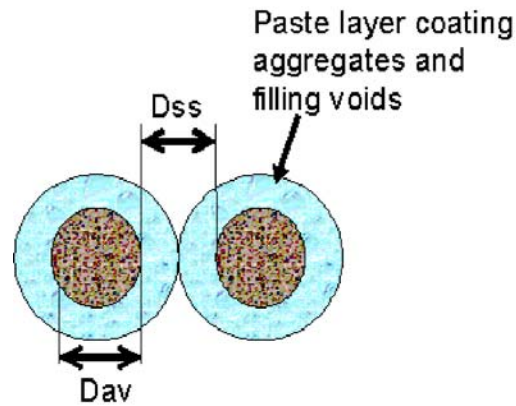


Figure 3.5: Minimum paste volume theory

It was proposed that the performance of the concrete could be predicted through characterization of the paste matrix. The paste rheology was assumed to be independent on the density difference between the aggregate and the matrix, D_{ss} , D_{av} , and the void content. D_{av} is computed from the particle size distribution and is given by:

$$D_{av} = \frac{\sum d_i m_i}{\sum m_i} \quad \text{Equation 3.12}$$

where d_i is the average size of aggregate fraction “i” and m_i is the percentage of mass retained between the upper and lower sieve sizes in fraction “i”. D_{ss} is a function of the void content, average diameter, and aggregate volume (paste volume), and the void content (V_{void}) is determined by measuring the volume of voids in the compacted aggregate (modified ASTM C-39) . D_{ss} is given by:

$$D_{ss} = D_{av} \left\{ \sqrt[3]{1 + \frac{V_p - V_{void}}{V_c - V_p}} - 1 \right\} \quad \text{Equation 3.13}$$

where V_c is the total concrete volume. It was assumed that the $\Delta\rho$ for the different mixes would be small, and hence this factor was neglected in the model.

In order to develop the model, the performance of the fresh SCC concrete was designed to have either poor segregation resistance and poor deformability or satisfactory deformability and segregation resistance. The paste rheological properties were quantified using viscosity and paste flow (Sections 3.3.3 and 3.3.4) and compared with the fresh concrete performance in order to determine the minimum flow and viscosity needed to produce satisfactory SCC. The paste flow was used in this model instead of the yield stress because previous studies have shown that it is possible to obtain a negative value for the yield stress of some SCC pastes when they are modeled as a Bingham fluid (Bui, Akkaya et al. 2002). A negative yield stress is an indication that the mix does not follow the Bingham model and the Power law may be a more accurate model for the behavior of these paste mixtures (Tang, Yen et al. 2001; Bui, Akkaya et al. 2002). Several studies have been conducted to determine if slump drops (slump flows) accurately reflect the rheological properties of concrete. In the slump test, the concrete will move only when the yield stress of the concrete has been exceeded; hence, the slump test is related to yield stress (Ferraris 1999). Work conducted by Scullion showed that the slump has a negative power law dependence on yield stress and that this relationship is largely independent of viscosity (Tattersall 1976). In 2000, using a generalized dimensionless approach, Saak concluded that the fundamental relationship between yield stress and slump is independent of the material and largely independent of the slump cone geometry. Studies have also shown that the slump flow of paste is also related to yield stress (Kokado 1999; Ichimiya, Idemitsu et al. 2000) and hence, it was decided use the paste flow as an indication of the yield stress.

It was determined that, for a given aggregate diameter there is always a minimum value of paste flow below which the concrete always exhibited poor deformability (Figure 3.6). Similarly, there is a minimum value of paste viscosity below which the concrete mixtures always exhibited poor segregation resistance (Figure 3.7). However, mixtures that were above the minimum flow line did not always have good segregation resistance, and mixtures above the minimum viscosity line did not always have good deformability. Hence, it was determined that the flow and viscosity could not be varied independently, and instead the researchers proposed that there is an optimum flow/viscosity ratio that must be considered for good deformability and segregation resistance. This theory was verified by plotting the flow/viscosity ratio vs D_{ss} (Figure 3.8). From this plot, it was apparent that distinct curves separated the segregation, satisfactory and low deformability zones. Hence, the flow/viscosity ratio is the governing factor in determining the area of the self-flow zone (Figure 3.9).

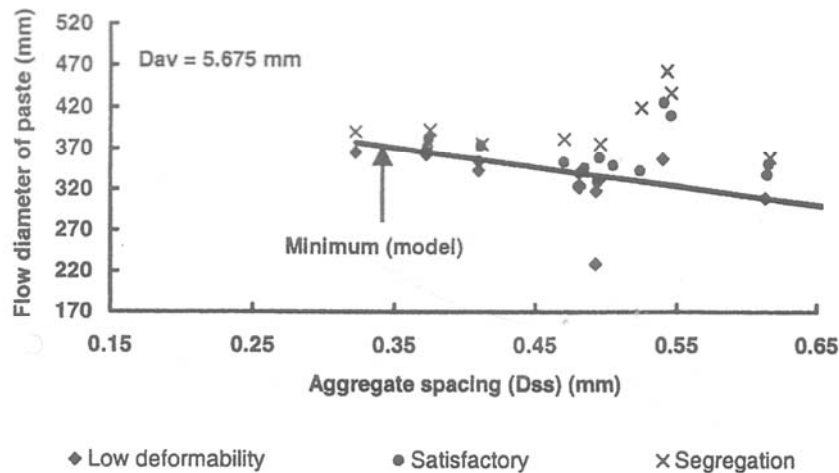


Figure 3.6: Minimum line for paste flow (Bui, Akkaya et al. 2002)

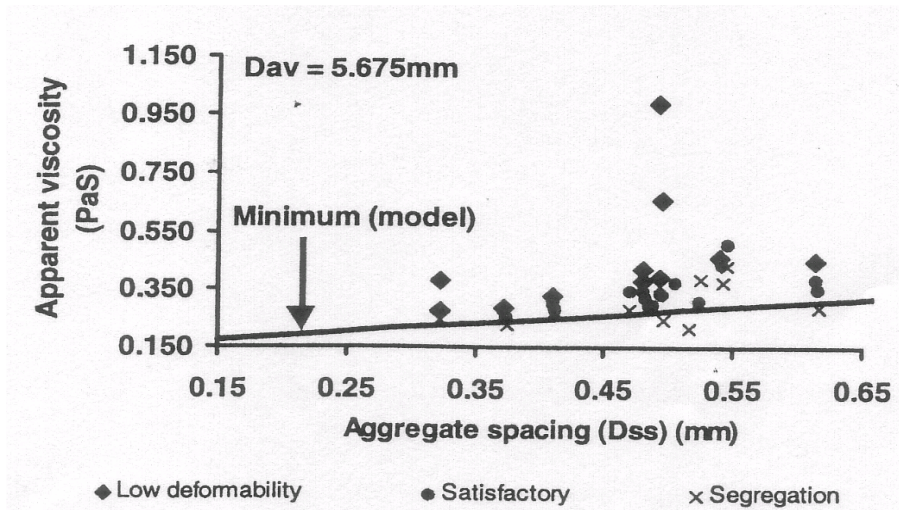


Figure 3.7: Minimum line for viscosity (Bui, Akkaya et al. 2002)

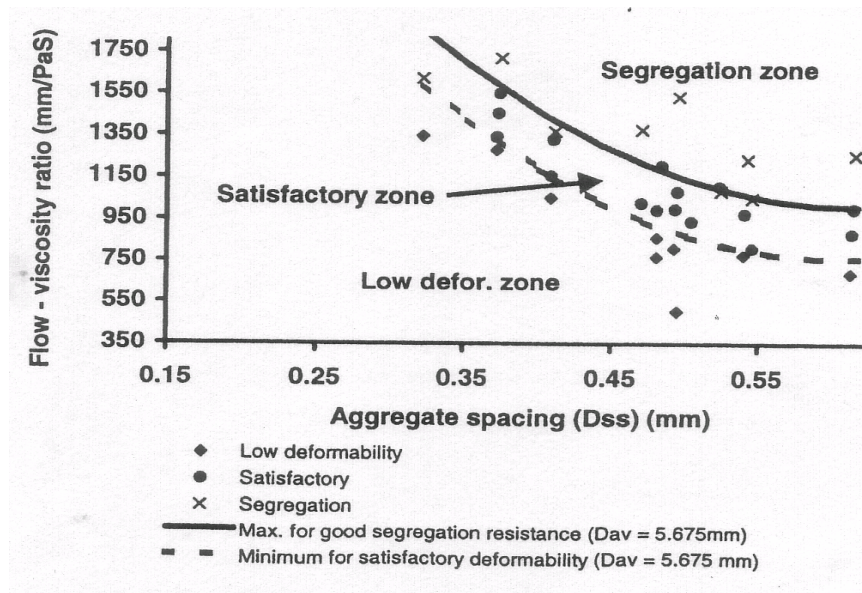


Figure 3.8: Model lines (Bui, Akkaya et al. 2002)

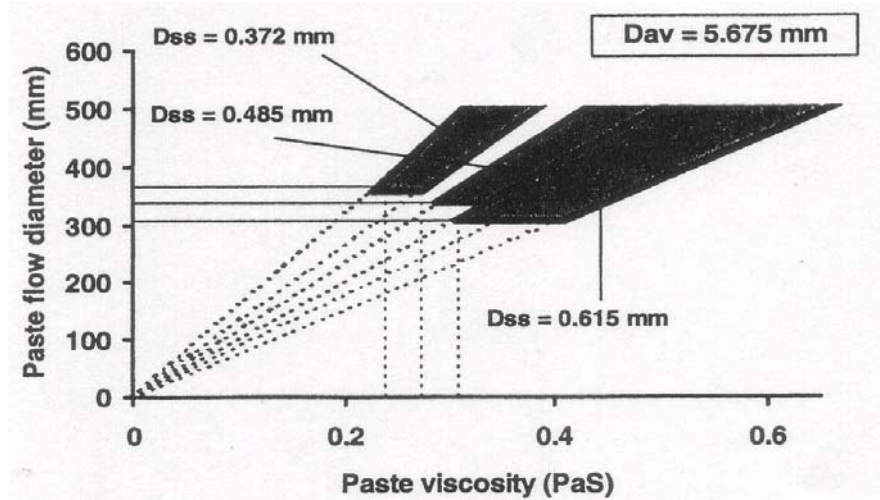


Figure 3.9: Satisfactory zone obtained from combination of minimum flow diameter, minimum viscosity, and optimum flow/viscosity ratio(Bui, Akkaya et al. 2002)

This model was originally developed by testing over 60 concretes mixes and over 74% of those mixes had w/b ranging from 0.38-0.40. However, the concrete mixes in this study have w/b of 0.35 and 0.45. Therefore, a study was conducted in order to determine if the model is valid for a wider range of concrete mixes.

3.3 Experimental Program

3.3.1 Materials

The paste mixes in this chapter corresponds to the concrete mixtures used Section 2.3.6. The paste volume resulting from 1.2L of the concrete was used to develop the mixture proportions (Table 3.2).

Table 3.2: Paste Mix Proportions

Mix	Cement (kg)	FA (kg)	Water (kg)	SP (kg)
S35-F0	0.619	0.000	0.217	0.00255
S35-F20	0.479	0.120	0.210	0.00180
S35-F30	0.413	0.176	0.206	0.00147
S45-F0	0.538	0.000	0.243	0.00255
S45-F20	0.418	0.105	0.236	0.00255
S45-F30	0.361	0.155	0.233	0.00255

3.3.2 Mixing Protocol

All mixes were prepared by placing the water into a standard Hobart planetary mixer. The cement and fly ash were weighed out together and added to the mixer over a one minute interval. The paste was mixed for 2.5 minutes at speed 1. Then, the mixer was stopped and the sides of the mixing bowl were scraped over a 30 second interval. During a 10 second interval the superplasticizer was added to the paste and then the paste was mixed at speed 2 for an additional 2.5 minutes. Immediately, after mixing a portion of the paste was placed into a HAAKE-RS150 rheometer for viscosity testing and flow of paste tests were conducted.



Figure 3.10: Paste flow diameter

3.3.3 Flow test

A mini-cone and glass plate was used to measure the flow of paste. The dimensions of the cone are 70 mm, 100mm, and 50 mm, for the upper inner diameter, lower inner diameter, and height. The cone was placed in the center of the glass plate, and after mixing the paste was poured into the cone. Then, the cone was lifted and the diameter at two perpendicular directions were measured after the paste stopped flowing (Figure 3.10). The average diameter from these two measurements was used as the slump flow.

3.3.4 Viscosity

The same protocol used by Bui et.al was used in this study. The viscosities of the pastes were measured using a concentric cylinder rheometer. For all samples, a pre-determined volume was poured in the rheometer. During a 10 second time interval, the shear rate was ramped up from 0 s^{-1} to 600 s^{-1} . Then the shear rate was held constant at 600 s^{-1} for a period of 120 seconds. Finally, the shear rate was ramped down from 600 s^{-1} to 0 s^{-1} over a 30 second interval. The apparent viscosity from the up curve taken at a shear rate of 100 s^{-1} was used in the analysis.

3.4 Results and Discussion

3.4.1 Comparison with Rheological Model

All the mixes were designed with the same coarse/total aggregate ratio and aggregates in order to eliminate differences in the void content and D_{av} . The void content and D_{av} was determined as 20.2 % and 5.675 mm, respectively. This corresponds to a D_{ss} of 0.45 mm. The test results for flow diameter, viscosity, and flow-viscosity ratio are presented in Table 3.4 and Figures 3.11 -3.14. The minimum lines depicted in Figures 3.6 – 3.8 indicates the limit for a satisfactory SCC. The limit values were obtained from the previous study by Bui et.al.

3.4.1.a Paste Flow Diameter

Previous studies have shown that the stress vs. shear rate of paste for SCC follows the Power Law or Herschel-Bulkey model, and not the Bingham relationship (Tang, Yen et al. 2001). Hence, the paste flow, which appears partly related to the yield stress, was used as an indicator of the concrete's yield stress. Higher values for paste flow correspond to lower values of yield stress. According to the rheological model (Bui, Akkaya et al. 2002), for a D_{ss} of 0.45 mm a minimum flow diameter of 347 mm is needed in order to have a SCC with good deformability. All of the mixes meets this criterion. In addition, although mix S45-F0 has a paste flow higher than the minimum flow, the respective concrete exhibits a little honeycombing. This confirms the findings of a previous study (Bui, Akkaya et al. 2002) that meeting the minimum paste flow does not guarantee good mold-surface finishing of concrete (see also further discussion in Section 3.4.1.d.)

3.4.1.b Apparent Viscosity

Replication testing for viscosity measurements was performed on each mix, and the results are shown in Table 3.3. As expected, there is some degree of experimental error due to the sensitive nature of test.

Table 3.3: Repeatability testing for viscosity

Mix	S35-F0	S35-F20	S35-F30	S45-F0	S45-F20	S45-F30
Viscosity (Pa.s)	0.359	0.299	0.333	0.117	0.109	0.084
	0.388	0.291	0.29	0.149	0.106	0.118
	0.322			0.178	0.113	0.106
Ave. Viscosity (Ps.s)	0.356	0.295	0.312	0.148	0.109	0.103
St. Dev. (Pa)	0.033	0.006	0.030	0.031	0.004	0.017

Table 3.4: Paste flow diameter and viscosity

Mix	Flow Diameter (mm)	Ave. Viscosity (Pa•S)	Flow/Viscosity (mm/PaS)
S35-F0	375	0.356	1071
S35-F20	388	0.295	1315
S35-F30	355	0.312	1137
S45-F0	496	0.148	3352
S45-F20	518	0.109	4752
S45-F30	522	0.103	5068

As expected, for a given w/b, the addition of fly ash decreases the viscosity. This supports previous findings (Tattersall and Banfill 1983; Ferraris, Karthik et al. 2001) that there are rheological benefits to using fly ash without increasing the superplasticizer dosage or increasing the water demand. According to the rheological model for a D_{ss} of 0.45 mm, a minimum apparent viscosity of 0.250 Pa•s is needed in order to have a SCC with good deformability and segregation resistance. All of the lower w/b mixes meet this criterion, but all of the higher w/b mixes have viscosities that fall below the minimum value. Hence the model predicts that these mixes will result in concrete that will segregate. The reason may be due to the fact that higher w/b mixes have a higher difference between densities of the paste and aggregates (see further discussion in section 3.4.1.d).

3.4.1.c Optimum Flow-Viscosity Ratio

According to the rheological model, for a D_{ss} of 0.45 mm the lower and upper bounds for a good quality SCC is 1006 mm/Pa•S and 1279 mm/Pa•S, respectively. These values were used to determine the satisfactory zone depicted in Figure 3.11. From this plot, the previous study predicts that the higher w/b mixes would produce a concrete that is prone to segregate, and the lower w/b mixes are likely to produce a good quality SCC.

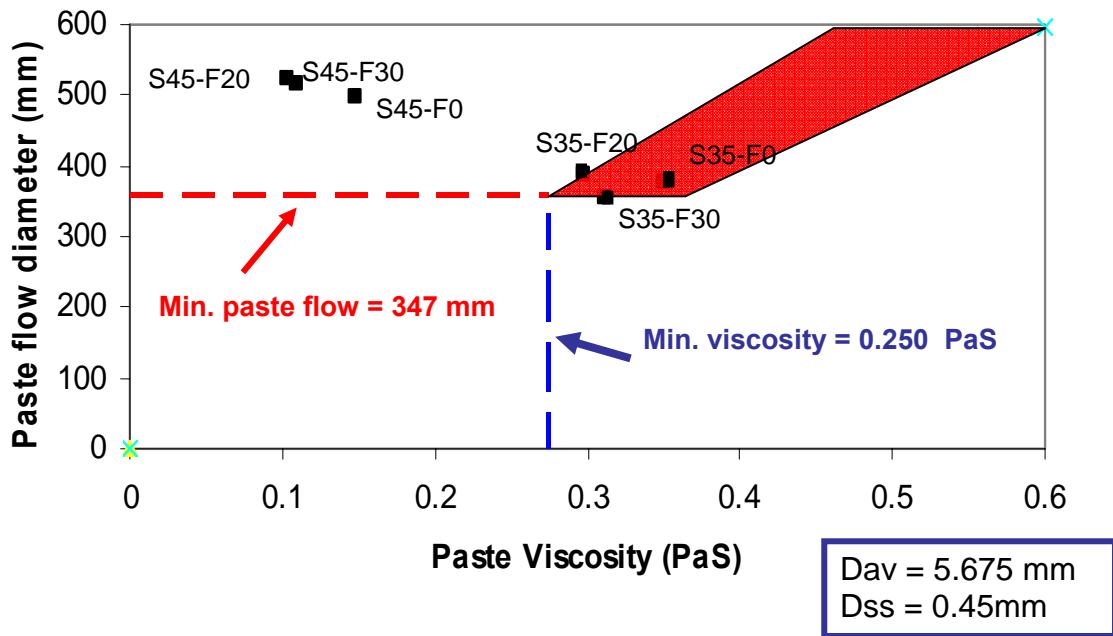


Figure 3.11 Self flow zone (shaded in red). Minimum values were obtained from (Bui, Akkaya et al. 2002)

Hence, there is a discrepancy between the rheological model prediction for the concrete based on the cement pastes and the actual performance of the concrete determined from the testing methods described in Section 3.3.2. According to the model, for the given paste flow diameters, the viscosity of the higher water/binder mixes should be in the range of about 0.35 – 0.50 Pa•S. Thus, the difference between the model predications and the actual experimental results appears to be related to the low viscosity values for the high w/b mixes. Several experimenters have reported the existence of slippage (Saak 2000; Struble, Puri et al. 2001), sedimentation when using concentric cylinders rheometers for water/cement ratios over 0.40 (Bhatty and Banfill 1982; Tattersall and Banfill 1983) and centrifugal separation (Tattersall and Banfill 1983). Although the viscosity values listed in Table 3.4 appear to be low, they are within the 50-fold range reported by Tattersall and Banfill (Tattersall and Banfill). Therefore, it is possible that the true tendency of viscosities of the mixes is being captured. However, it is well known that

measurement procedure influences the rheological properties of cementitious based materials (Ferraris, Karthik et al. 2001; Geiker, Brandl et al. 2002) and as a result, the viscosity of the mixes were also compared against the viscosities determined from using a protocol based on the equilibrium method (Figure 3.12). In addition, modifications on the hysteresis loop measurements were also done (hysteresis loops with and without an equilibrium period, and decreasing the maximum shear rate for the hysteresis loop testing). The combined approach uses the peak stress in order to determine the plastic viscosity, whereas the viscosities from the equilibrium approach were computed using the equilibrium values. Hence, it is expected that the two approaches would yield different viscosity values due to the structural breakdown, and this trend was seen in the results. Similar viscosities were obtained using the different methods for S45-F30 and S35-F20, and this is a possible indication that slippage or sedimentation may be occurring during the combined approach method.

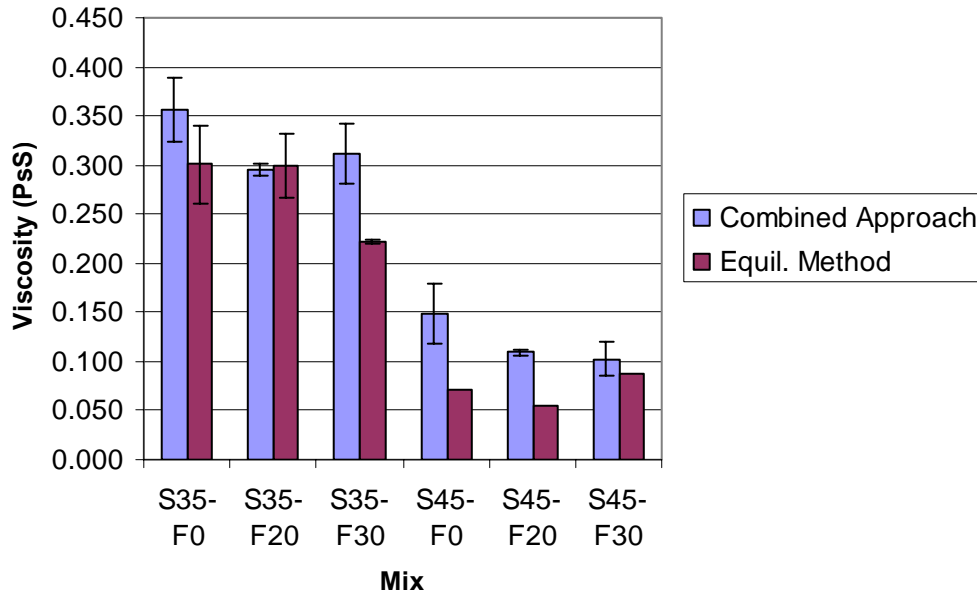


Figure 3.12: Viscosity comparison using combined approach and equilibrium approach

Although the previous model does an adequate job of predicting the performance of the lower water/binder mixes, in order to make it more robust

for a wider range of concrete, additional factors such as the difference between densities of paste and aggregates (i.e. the volumetric ratio between solid particle and liquid phase) need to be considered. Further discussion about this effect is in the following section.

3.4.1.d Effect of difference between densities of aggregates and paste

It was shown in Section 3.2.2.a, that for a single spherical particle, the segregation resistance under dynamic conditions is related to falling velocity (v) of the particle in a matrix (Equation 3.9), and it can be seen that a higher product between $\Delta\rho$ and r_a leads to a higher falling velocity. In order to avoid segregation, the falling velocity (v) should be minimized.

In the previous work (Bui, Akkaya et al. 2002), the models for minimum paste flow, minimum viscosity, and optimum paste flow-viscosity ratio were developed. These criteria are related to average aggregate spacing (D_{ss}) and average aggregate diameter (D_{av}) (see Figures 3.5-3.7). As mentioned, difference between densities of aggregates and paste ($\Delta\rho$) affect the correlation of paste rheology with fresh SCC's properties; however, this effect was neglected in previous work since the density difference ($\Delta\rho$) was small for the tested mixes. There is a bigger difference between the $\Delta\rho$ in this study and the $\Delta\rho$ in the previous study, and therefore $\Delta\rho$ can not be neglected. The average values of D_{av} , $\Delta\rho$, and product between average aggregate radius (r_{av}) ($r_{av} = D_{av}/2$) and $\Delta\rho$ of mixes in previous works and new tests are indicated in Table 3.5. The effects of the product between $\Delta\rho$ and r_{av} are illustrated in Figures 3.13, 3.14, and 3.15. The product between $\Delta\rho$ and r_{av} hereafter is noted as $P_{\Delta r}$.

Table 3.5: Product ($P_{\Delta r}$) of $\Delta\rho$ and r_{av}

Experiment Series	Coarse/total aggregate ratio (Nga)	D_{av} (mm)	$\Delta\rho$ (kg/m ³)	$P_{\Delta r}=\Delta\rho*r_{av}$ (g/m ²)
Previous experiment –Case A	0.40	4.673	0.839	1.960
Previous experiment –Case B	0.52	5.675	0.830	2.355
New tests-w/b=0.35	0.52	5.675	0.814	2.310
New tests-w/b=0.45	0.52	5.675	0.926	2.628

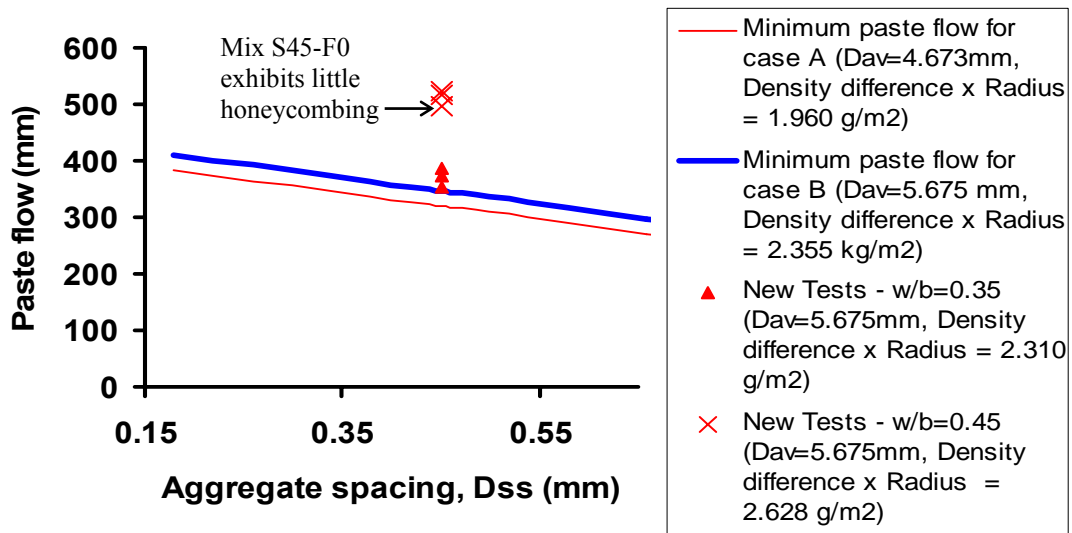


Fig. 3.13: Paste flow and different products of $\Delta\rho$ and average radius (r_{av}) of aggregate

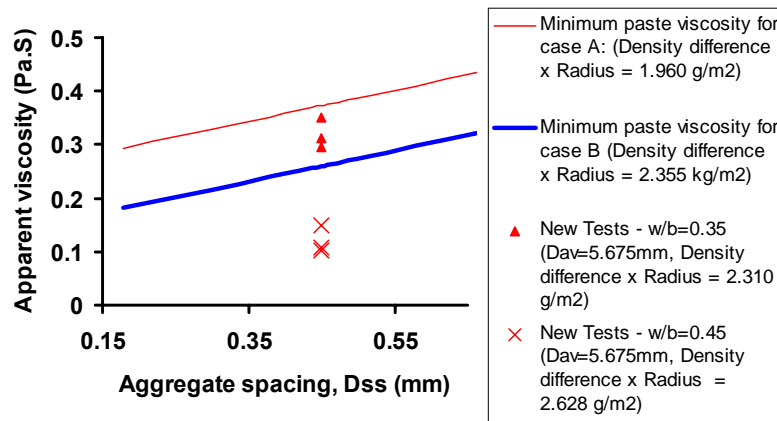


Fig. 3.14: Viscosity and different products of $\Delta\rho$ and average radius (r_{av}) of aggregate

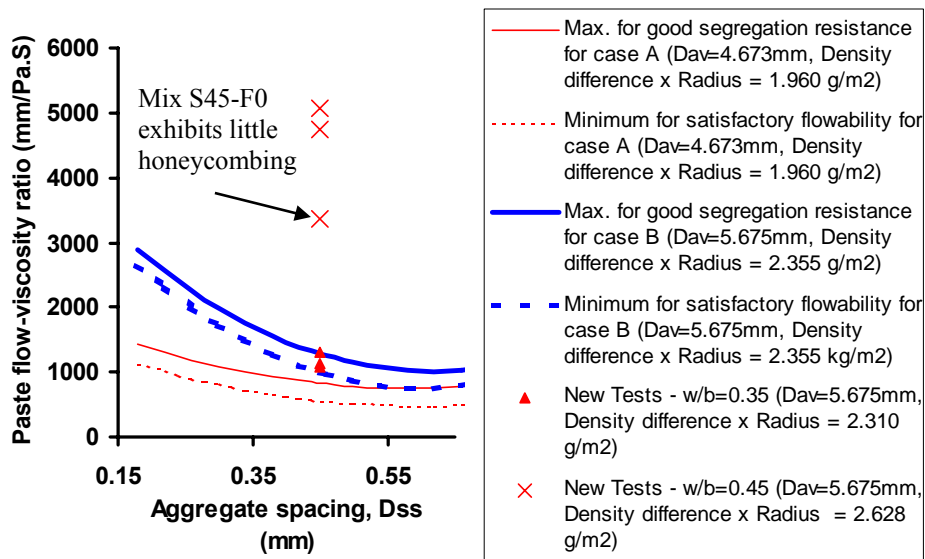


Figure 3.15: Paste flow-viscosity ratio and different products of $\Delta\rho$ and average radius (r_{av}) of aggregate

Figures 3.13 and 3.14 indicate that, for the same aggregate spacing, higher values of $P_{\Delta r}$ tend to increase the minimum paste flow required in order to achieve good flowability of SCC, and decrease the minimum viscosity needed to avoid segregation of concrete. Figure 3.15 shows the tendency that, for a

given aggregate spacing, greater values of $P_{\Delta r}$ require a greater paste flow-viscosity ratio in order to achieve satisfactory flowability and good segregation resistance of SCC. The test's results suggest that there is a close relation between optimum paste flow-viscosity ratio and falling velocity (v) as seen in Equation 3.9 since higher values of $P_{\Delta r}$ also results in greater falling velocity in order to avoid segregation of a particle in a matrix. From Equations 3.9, 3.10, and 3.11, it can be shown that the falling velocity of the mix is proportional to $P_{\Delta r}$ and inversely proportional to matrix viscosity.

$$v^2 \propto \frac{P_{\Delta r}}{\eta} \quad \text{Equation 3.14}$$

If the falling velocity is assumed to be a constant, then the viscosity of the matrix should decrease as $P_{\Delta r}$ increases, and this trend was evident in the study. However, since the self-flow zone is characterized by the flow/viscosity ratio, low viscosity values can lead to extremely high flow/viscosity ratios. As previously mentioned, the flow of paste is related to yield stress and SCC mixes are generally designed with low yield stress values and the segregation resistance is primarily controlled by the matrix viscosity. The range for paste flow is much smaller than the possible range for viscosity, thus resulting in large values for the flow/viscosity ratio when the viscosity of the mixes decreases. A plot of the flow/viscosity ratio versus $P_{\Delta r}$ (Figure 3.16) indicates that the that the flow/viscosity ratio is proportional to $(P_{\Delta r})^2$. Recall that the area of the self-flow zone is determined by the flow/viscosity ratio, and it is interesting to see that both the relationship between the flow/ratio and $P_{\Delta r}$ and the relationship between $P_{\Delta r}$ and the falling velocity is a function of the second power. This supports the notion that $P_{\Delta r}$ is an important parameter in determining the self-flow zone of SCC.

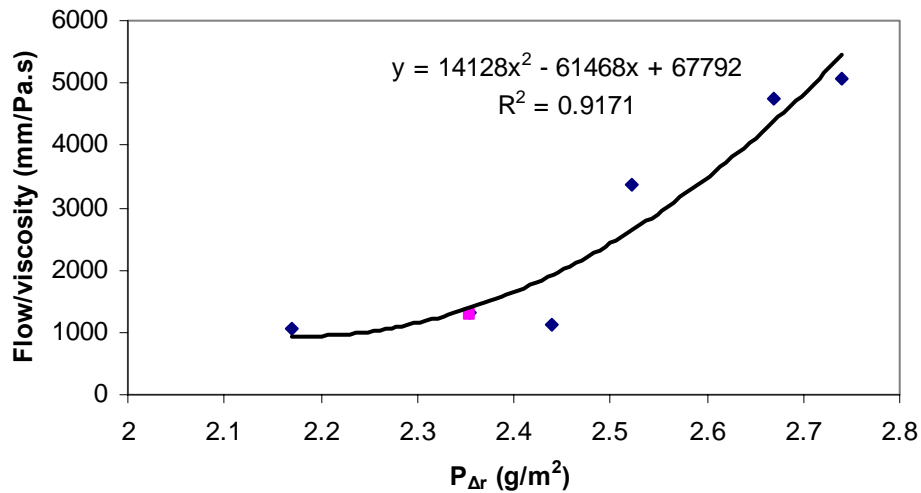


Figure 3.16: Relationship between flow/viscosity ratio and $P_{\Delta r}$

However, in order to confirm this hypothesis, and incorporate the effect of $P_{\Delta r}$ into a universal model, further study is needed.

3.5 Summary

The flow behavior of cementitious materials is often described using the Bingham model, and the yield stress and viscosity are critical parameters that should be considered in the design of SCC. This chapter introduced the concept of rheology and discussed how the key properties of SCC are influenced by the yield stress and viscosity. In addition, the “self-flow zone” design methodology and a paste rheology method that uses the concept of minimum paste volume were briefly discussed. The paste rheology model was used to characterize the paste matrix of the concretes developed in Chapter 2, and the results from the model were compared with the fresh state results from Chapter 2. The model does an adequate job of predicting the performance of the S35 mixes, but for the higher w/b, the effect of difference between densities of aggregates and paste cannot be neglected. It was determined that both aggregate spacing (D_{ss}) and the product ($P_{\Delta r}$) between average aggregate

radius and difference between densities of aggregates and paste influence the correlation of paste rheology with fresh SCC's properties. A further study is needed to investigate the influence of difference between densities of paste and aggregates, and the behaviors of possible slip, sedimentation, or centrifugal separation when determining the viscosity using a concentric cylinder rheometer.

In the next chapter, the hardened state properties of the concrete developed in Chapter 2 are evaluated. .

Chapter 4: Hardened Properties

4.1 Introduction

In Chapters 2 and 3, the fresh state properties were evaluated, however hardened state properties, such as compressive strength and durability, are also important material properties and therefore they should be tested. In structures with congested reinforcement or restricted spaces, it is often difficult to consolidate concrete through vibratory methods, and inadequate compaction of concrete can dramatically decrease the strength and durability of mature concrete, and SCC was developed as a means to ensure adequate consolidation of in-situ concrete, thus guaranteeing homogeneity in the hardened state.

A discussion of the compressive strength and permeability of SCC, as well as the testing methods used to evaluate these properties will be given in this chapter. This chapter also presents the results from the testing methods and general conclusions about the effect of fly ash on the compressive strength and permeability are made.

4.2 Background

4.2.1. Compressive Strength

It is well known that concrete is weak in tension and strong in compression. As a result, the compressive strength of concrete is often considered the most important property of concrete, and is the most common measure used to evaluate the quality of hardened concrete (Mather and Ozyildirim 2002). Compressive strength can be defined as “the measured maximum resistance of a concrete specimen to axial loading” (Kosmatka, Kerkhoff et al. 2002), and is determined by computing the maximum stress (f'_c) that the specimen carries after being subjected to uni-axial compressive force. In North America, the standard test specimen is a cylinder with a length

to diameter (l/d) ratio of 2. The stress values can be obtained by dividing the experimental load (P) by the cross-sectional area (A) of the specimen. For the geometry shown in Figure 4.1 $A = \frac{\pi d^2}{4}$.

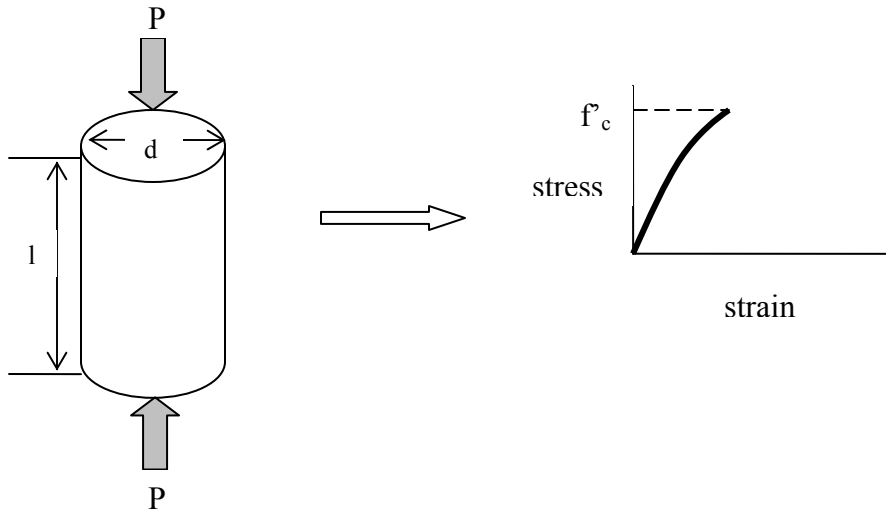


Figure 4.1 Compressive Strength Test Schematic

Principal factors governing the compressive strength of concrete are the water/cement (w/c) ratio, curing conditions, age of the concrete, cementitious material, aggregates, mixing time, degree of consolidation, and air content (Mather and Ozyildirim 2002). When fly ash is used as a replacement for Portland cement, the compressive strength during the first 28 days is normally lower due to the slower nature of the pozzolanic reaction. Depending on the mix proportions, concrete containing fly ash may require 28 to 90 days to exceed the 28-day control strength (Kosmatka, Kerkhoff et al. 2002). Hence the addition of fly ash has the effect reducing early strength, but not the long term strength and fly ash has been used in the production of high strength concrete (exceeding 100 MPa). The relationship between the w/c and compressive strength of concrete has been extensively studied and research

has shown that the compressive strength is inversely proportional to w/c (Figure 4.2). In 1948, Powers and Brownyard (Mindess, Young et al.) determined that this relationship was due to the influence of the capillary porosity of the cement paste. Porosity is a measure of the amount of voids in concrete and it is directly proportional to the w/c ratio.

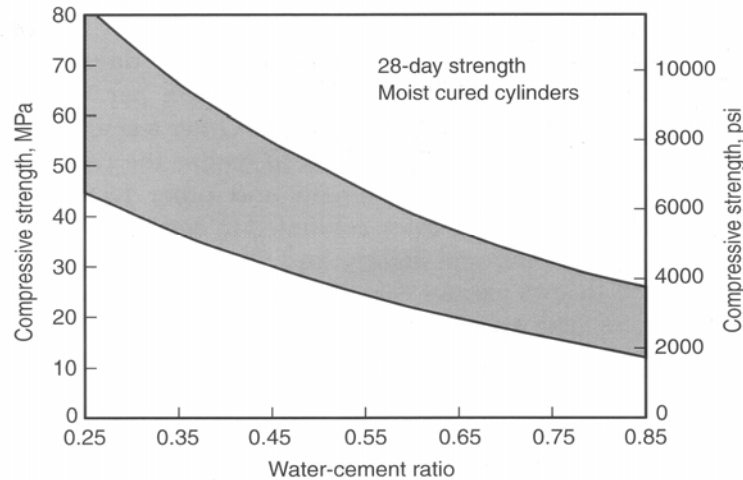


Figure 4.2: Range of typical strength to w/c ratio relationships of concrete based on over 100 different concrete mixtures (Kosmatka, Kerkhoff et al. 2002)

Numerous studies have been conducted to evaluate the compressive strength of SCCs. Gibbs and Shu (Gibbs and Shu) tested the compressive strength of SCC mix (w/c=0.71) and a reference NVC (w/c=0.68) in standard laboratory specimens and full-scale columns. In the standard laboratory specimens, the 28-day strength and the rate of strength development were similar for SCC and NVC. However, less variation was found between the compressive strength of the standard specimens and the full-scale column for the SCC mixes. A database evaluating the results of a large number of internationally published data on properties of SCC was created by Klug and Holschemacher (Klug and Holschemacher). Through analysis of the database, it has been concluded that for a given w/b, the compressive strength and the strength development of SCC and NVC are similar.

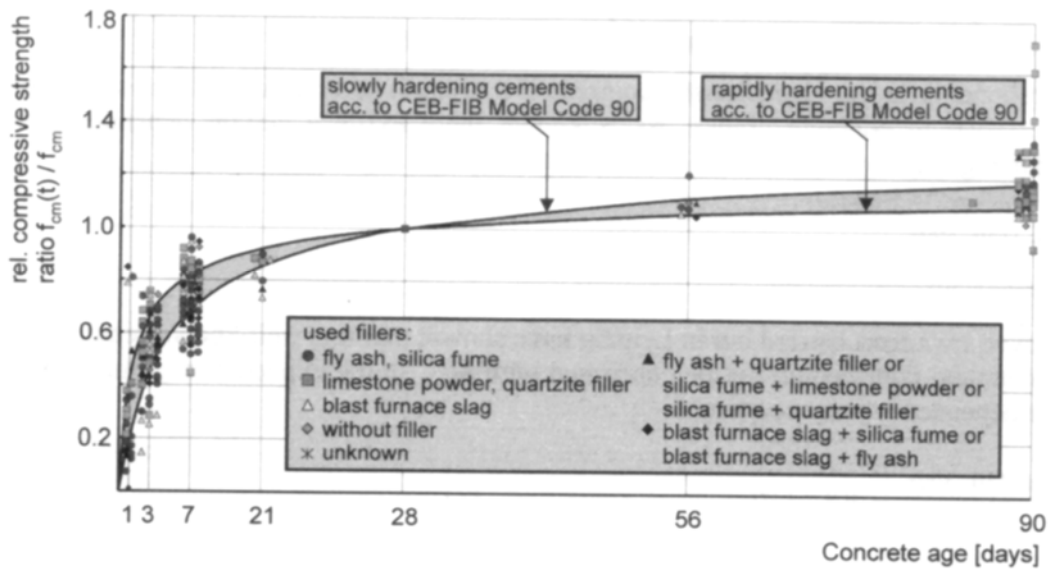


Figure 4. 3: Compressive Strength Development of SCC with time in comparison with the regulations of Model Code 90 (Klug and Holschemacher 2003)

Compressive strength is not an intrinsic material property and it is affected by specimen geometry, specimen preparation, moisture content, temperature, loading rate, testing loading fixture, and type of testing machine (Mindess, Young et al. 2003). In order to minimize the variability that would occur from using different test procedure, standardized tests have been developed. ASTM C39 is the standardized test used to evaluate the compressive strength concrete in North America.

4.2.2. Permeability

It is well known that the ability of concrete to resist deterioration from chemical and environmental attack can be directly related to its permeability. Permeability is defined as the rate of flow of moisture through concrete under a pressure gradient (Mather and Ozyildirim 2002). As the water/cementitious ratio is increased, porosity increases, and hence the concrete becomes more permeable. A permeable concrete is more susceptible to ion penetration (which can lead to corrosion of metals—usually steel reinforcement), to

stresses that are induced by the expansion of water as it freezes, and to chemical attack (leaching, efflorescence, sulfate attack). If properly cured, most concretes become significantly less permeable with time. Therefore, it is important to specify the age at which the permeability is measured.

Various methods (both direct and indirect) have been developed to evaluate the permeability of concrete and these methods generally fall into three categories: air permeability, water permeability, and chloride permeability. The most common methods for determining the permeability of concrete are: chloride ponding test (AASHTO T259), air and water permeability tests (ACI 228.2R), hydraulic permeability by the American Petroleum Institute (API RP 27), and the rapid chloride permeability test (RCPT) (ASTM C1202 or AASHTO T 277). The RCPT method is the fastest method of those mentioned and is often used for specification and quality control purposes. Chloride permeability is of particular concern in considering the durability of reinforced concrete structures since chloride ions have the ability to destroy the passive oxide film that coats the rebar surface. Once this layer is destroyed, moisture and oxygen can gain access to the rebar and the formation of rust will occur. The RCPT test, also known as the electrical resistance test, was originally developed by Whiting in 1981. This six hour test provides a rapid indication of concrete's resistance to the penetration of chloride ions by monitoring electric current across the specimen. A voltage of 60V DC is maintained across the ends of the sample throughout the test. The more permeable the concrete is, the more chloride ions will migrate, and the higher the current will be. The concretes are qualitatively using the criteria in Table 4.1(ASTM C1202-97).

Table 4.1: Chloride Ion Penetrability Test (RCPT)

Chloride Permeability	Charge passed (Coulombs)	Representative type of concrete
High	>4000	High water-cement ratio (0.6)
Moderate	2000 – 4000	Moderate water-cement ratio (0.4-0.5)
Low	1000 – 2000	Low water-cement ratio “Iowa” dense concrete
Very low	100 – 1000	Latex-modified concrete Internally sealed concrete Microsilica concrete
Negligible	<100	Polymer-impregnated concrete Polymer concrete

Raghavan et al (Raghavan, Sarma et al.) compared the chloride permeability of SCC and NVC specimens at an age of 28 days using the RCPT method. They report lower coulomb values in the SCC specimens than the NVC specimens, and it is believed that this decrease in coulomb value (which means lower chloride permeability) is from a denser microstructure due to better compactness. It is well known that a denser microstructure can lead to improved concrete durability, and Raghavan et al. results confirm previous findings that reports a denser interfacial transition zone (ITZ) as well as a denser bulk paste in SCC compared to NVC (Tragardh 1999). Studies have also shown that SCC containing supplementary cementitious materials have a denser and more homogenous microstructure than NVC and SCC without supplementary cementitious materials (Westerholm, Skoglund et al. 2002). The addition of fly ash generally reduces the permeability of concrete, and tests have shown that the permeability of concrete decreases as the quantity of hydrated cementitious material increases (Kosmatka, Kerkhoff et al. 2002).

All methods used to evaluate permeability exhibit high variability, and although the RCPT method is widely used, the test has its drawbacks. Main criticisms against this method are:

- The movement of all ions, not just chloride ions, affects the test result (the total charge passed) and studies have shown that supplementary cementitious materials (such as fly ash or silica fume) or chemical admixtures (such as water reducers or superplasticizers) can create misleading results due to the chemical composition of the pore solution. (Stanish, Hooton et al.). ASTM C-1201 and AASHTO T-277 both contain a caution about interpreting test results from surface-treated concretes.
- Microstructural changes in the concrete can occur from temperature increases from the voltage application. The heating leads to a further increase in the current that leads to unrealistic total charge values.

Despite these limitations, since the RCPT method can be applied quickly, it is widely used by various state departments of transportation to evaluate concrete bridge decks and as a standard to evaluate new mix designs. Numerous studies have shown a linear correlation exists between the total charge and initial current measured for the RCPT method. In 1996, Wang et.al showed that this relationship existed independently of the w/c ratio (Figure 4.4).

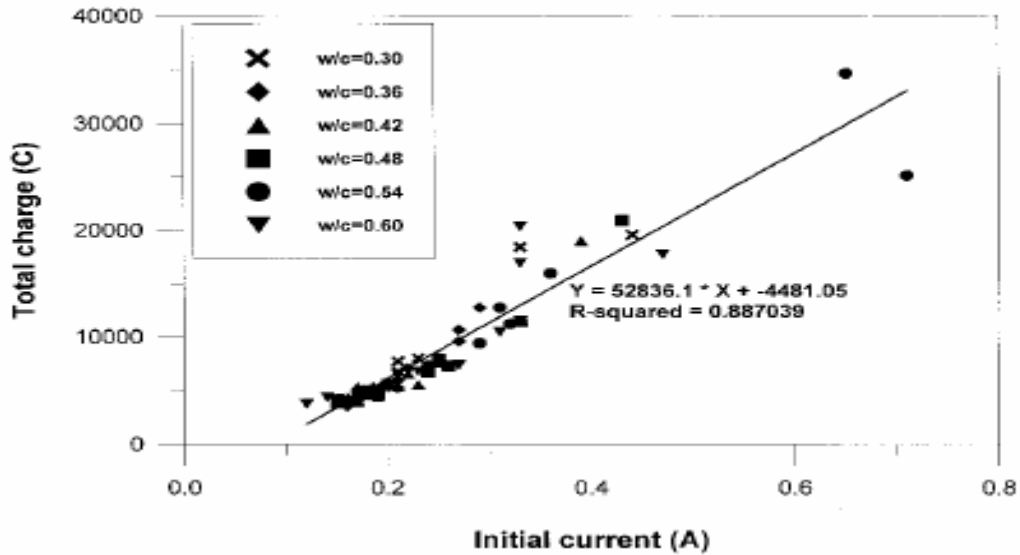


Figure 4.4 Relationship between total charge and initial current (Wang, Jansen et al. 1996)

In 1999, McGrath and Hooton (McGrath and Hooton) conducted a study in which the RCPT test was shortened to 30 minutes in order to eliminate the effects of specimen heating. Results from this study showed that the 30 minute test and the full 6 hour test yielded values within 10% at low charge values; however, larger differences occurred at higher charge values (Figure 4.5). At the same time, Shane et.al (Shane, Aledea et al.) reported the trend of deviation in the plot of initial current versus total charge from a theoretical line at values above 2000-4000 Coulombs (Figure 4.6). This theoretical line was obtained from the slope of the plot of the initial current versus total charge. For the RCPT test, the total charge is obtained by integrating the area under the current versus time plot, hence $Q = \int I dt$. At a constant current, the total charge is $Q = It$ where $t = 21600$ seconds and I is the initial current. Therefore, the theoretical slope of the plot of I versus Q is t^{-1} . For the RCPT test, the value of the theoretical slope is $4.63 \times 10^{-5} \text{ s}^{-1}$.

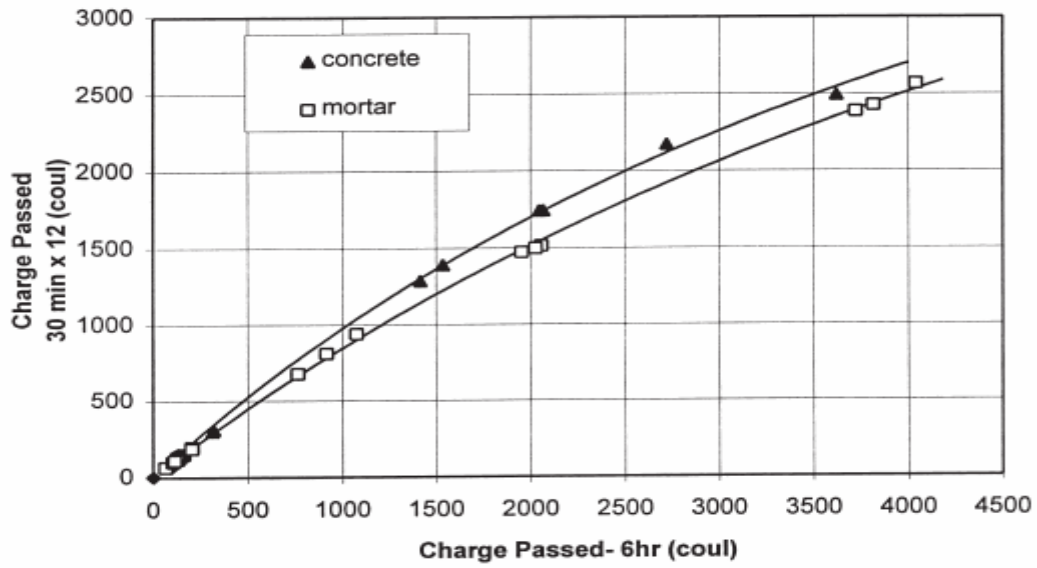


Figure 4.5 RCPT Plot of 6 hr charge vs. 30 min charge (McGrath and Hooton 1999)

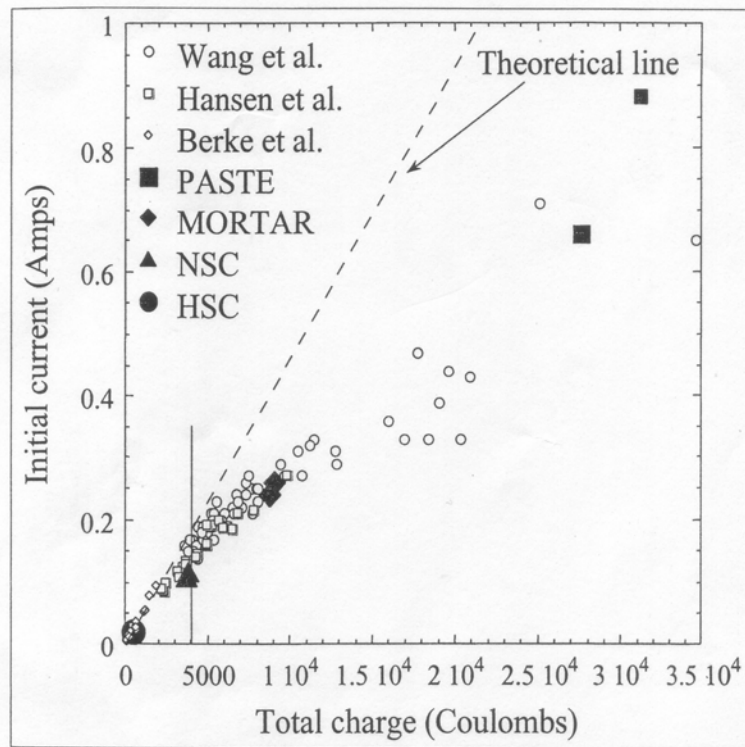


Figure 4.6 Initial current vs total charge for various researchers (Shane, Aledea et al. 1999)

4.3 Testing Methods

4.3.1. ASTM C39 (Compressive Strength)

Compressive strength testing was conducted at an age of one day, seven day, and twenty-eight days according to ASTM C39. The tests were performed with a MTS closed loop servo-hydraulic testing machine with a 4448 kN (1000 kip) capacity. A 489 kN (110 kip) load cell was used for the 1 day tests, and a 4448 kN load cell was used for the 7 and 28 days tests. Testing was performed in load control. Three specimens were tested for each mix, and the average of the three tests is used in the results.



Figure 4.7: Compressive test set up

4.3.2. RCPT

Specimens were prepared and testing according to ASTM C-1202 at 2 weeks and 16 weeks of age. Pictures of the test set-up are presented in Figures 4.8 and 4.9.

Sample Preparation: 4 x 8 in concrete cylinders were cured at 100% relative humidity until testing. Two-inch specimens were cut from the middle of the concrete cylinders and allowed to dry for at least an hour. Then, the lateral surface of the specimens was waterproofed with a rapid setting (~5-minute) epoxy. After the epoxy hardened the specimens were placed in a vacuum desiccator and the pressure was reduced to less than 1mm Hg (133 Pa). The vacuum was maintained for 2 hours. The separatory funnel was filled with de-aerated, de-ioned water and then the water trap was opened in order to allow the water to flow into the desiccator until the specimen was completely submerged. The vacuum was maintained for an additional hour before turning off the pump, and then the specimen was soaked under water for 18 hours.

Sample testing: Excess water was blotted off of the specimen after removing the specimens from the desiccator, and then the disks were clamped between a pair of test cells with steel rods. The boundary around the disk-cell was sealed with silicon adhesive and the adhesive was allowed to cure. Then each side of the cell was filled with either sodium chloride (3% by weight) or sodium hydroxide (0.3N) solution. The cell was connected to the testing machine with the positive wires to the sodium hydroxide solution and the negative wire to the sodium chloride solution. A thermal couple was placed in the test cell, and a direct voltage of 60 V was applied across the two faces. The monitoring of current and temperature were performed by the instrumentation and they were recorded at 30 minute intervals. For the specimens tested at 16 weeks of age, the test was stopped after 6 hours and the total charge was determined based on the trapezoidal rule shown below,

$$Q = 900(I_0 + 2I_{30} + 2I_{60} + \dots + 2I_{300} + 2I_{330} + I_{360})$$

where Q is the charge passed (coulombs), I_0 is the current immediately after the voltage is applied (amperes), and I_t is the current at “t” min after the voltage is applied (amperes). For the specimens tested at 2 weeks of age, the test was ceased after 100 seconds and the 100 second charge was extrapolated to estimate the 6-hour charge.

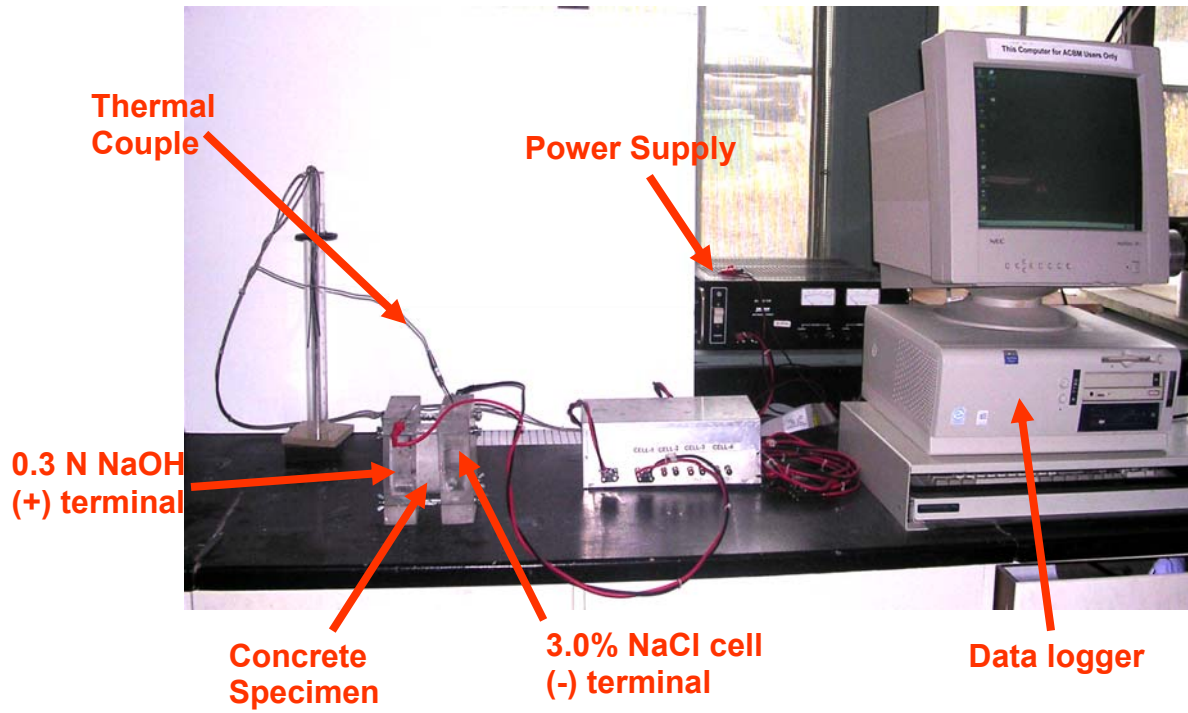


Figure 4.8 RCPT Test Setup

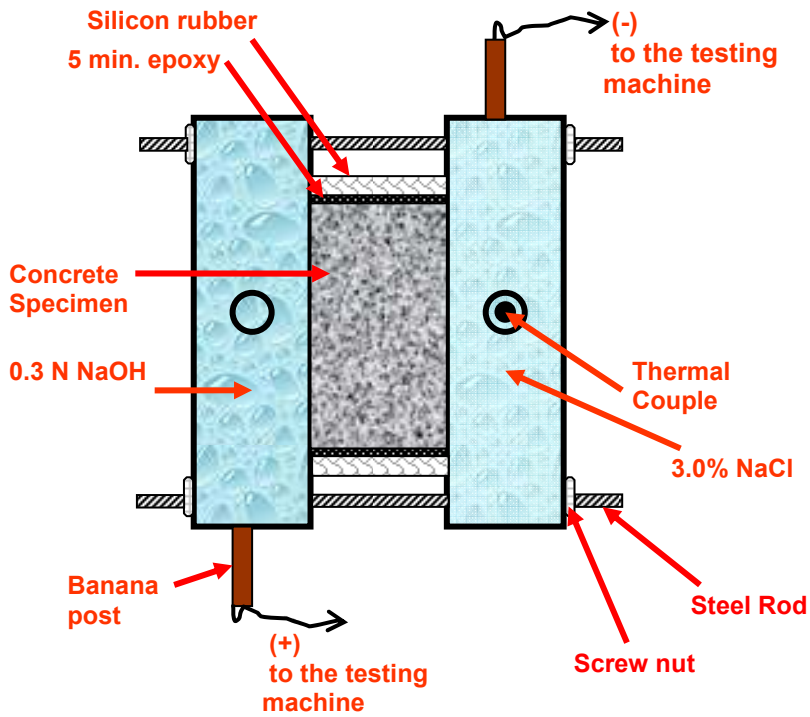


Figure 4.9 Top View of RCPT Set-Up

4.4 Results and Discussion

4.4.1. Compressive Strength

As expected, addition of fly ash resulted in a reduction of strength. However, all mixes still exhibited relatively high strengths, which ranged from 15 MPa to 35 MPa at 1 day, 37 MPa to 66 MPa at 7 days, and from 40 MPa to 70 MPa at 28 days. For the S35 mixes, fly ash substitutions of 20% and 30% decreased the early age strength by 5% and 40%, the 7 day strength by 21% and 40%, and the 28 day strength by 20% and 30%. For the S45 mixes, the addition of fly ash decreased the early age strength by 30% for both replacement percentages. Fly ash substitutions of 20% and 30% resulted in a reduction of 9% and 18% reduction in strength at 7 days. However, the strength reduction was only 13% at 28 days for both replacement ratios (Figure 4.9). For the lower w/b mixes, addition of fly ash also resulted in a greater reduction of strength compared with that of the control mix (S35-F0). The greater reduction in 28 day strength for the lower w/b ratio mixes is attributed to the decrease in the superplasticizer/binder ratio (Table 4.2). It is generally agreed that when superplasticizer is used to lower water requirements an increase in compressive strength will occur. This increase may be up to 25% greater than the strength that would have resulted from solely decreasing the w/c ratio (Mindess, Young et al. 2003). It is believed that the resulting strength increase may be due to a more homogenous microstructure from the dispersion of the cement and mineral admixtures. Hence, the decrease in strength in the lower w/b mixes containing fly ash may actually be an indication of a less uniform microstructure.

Early age strength development is of particular concern for contractors since it governs the time at which the formwork can be removed and reused. When forms are stripped the structure must be able to carry its own weight and any superimposed load. Walls and column forms are normally removed 12-24 hours after casting; but generally, formwork stripping is determined by the structural engineer based on the design strength of the concrete required for a particular project. For example, an engineer might specify that 40% of

the 28-day strength must be obtained prior to formwork removal. Ninety percent of ready mixed concrete is designed with a 28-day strength ranging from 20 MPa (3000 psi) to 40 MPa (6000 psi), and with the majority of the strength are between 28 MPa (4000 psi) and 35 MPa (5000psi) (Kosmatka, Kerkhoff et al.). Therefore, if a structure is designed for a compressive strength of 35 MPa and 40% of the 28 day strength is required prior to form stripping, the strength should be at least 14 MPa (2030 psi) before the formwork is removed. Even at the highest w/b ratio and highest fly ash replacement ratio, S45-F30 achieves a 1 day strength of 15.4 MPa (2234 psi), thus exceeding the minimum strength requirement for formwork. Hence, for typical structures, it is possible to achieve satisfactory early age strength using Class F fly ash made from Illinois coal. However, extra measures such as the use of Type III cement, reducing the w/c ratio, and/or additional heating or insulation is often taken to when rapid strength gain is desirable.

Compressive strength is inversely proportional to w/c ratio, and it can be expected that the strength development of S35-F0 (the mix with the lowest w/c ratio) would proceed faster than the other mixes. In general, the overall trend of strength development was similar for mixes with similar water/binder ratios.

Table 4.2 Superplasticizer/binder ratio

Mix	SP/binder
S35-F0	0.422
S35-F20	0.315
S35-F30	0.255
S45-F0	0.209
S45-F20	0.206
S45-F30	0.215

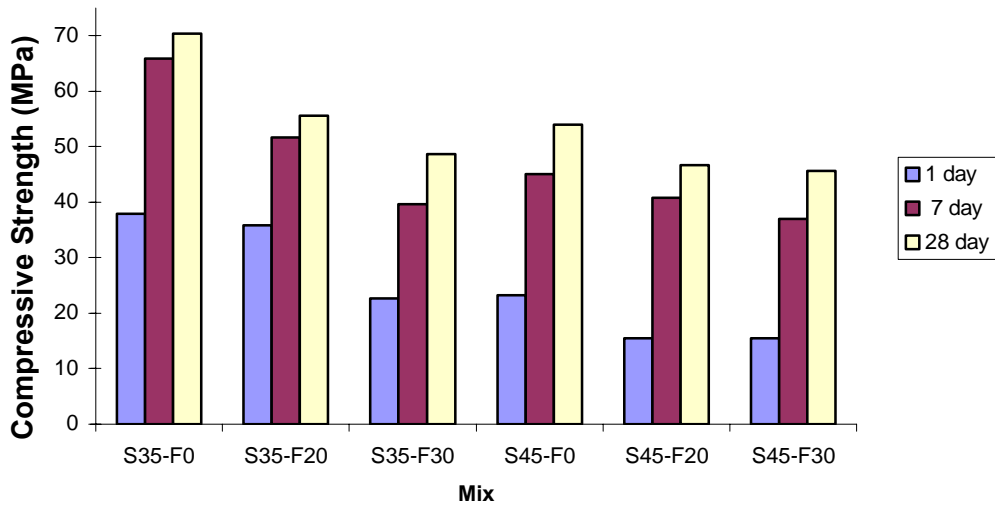


Figure 4.10: Compressive Strength Test Results

4.4.2. Permeability

Figure 4.10 shows the temperature versus time profile for the concrete specimens tested at 16 weeks of age. Final temperatures were elevated for all specimens, but the temperature increase was more significant for specimens without fly ash. After only one hour of testing S35-F0 and S45-F0 were experiencing temperatures of 80°F, and at the end of these specimens were experiencing temperatures of 106°F and 117°F, respectively. In general, the results show that differences between initial and final temperatures are considerably smaller for mixes incorporating fly ash. Final temperatures were similar for all mixes containing fly ash, and increasing the fly ash replacement ratio did not significantly affect the rate of temperature development. It is commonly accepted that prolonged exposure to high temperatures can damage the microstructure of concrete and one way to circumvent this effect is to reduce the duration of time in which the charge is applied.

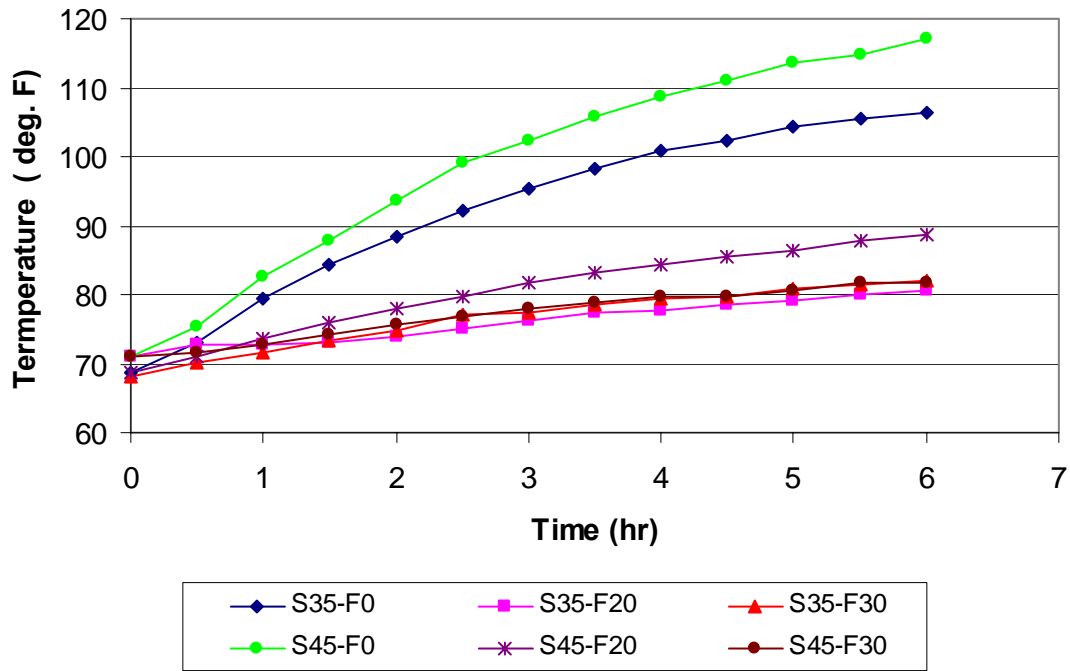


Figure 4.11 Temperature profile

As shown in Figures 4.5 and 4.6, many investigators have shown a good correlation between the total charge (Q) versus the initial current (I_0) for NVC; however, results have indicated a deviation from the best fit line and a large amount of scatter at high charge values. In order to investigate if this correlation also existed for SCC, the initial current at $t=100$ seconds versus the total charge was plotted for SCC specimens tested at 16 weeks of age (Figure 4.11). The results show that SCC mixes with fly ash also exhibit the same linear relationship between initial current and total charge.

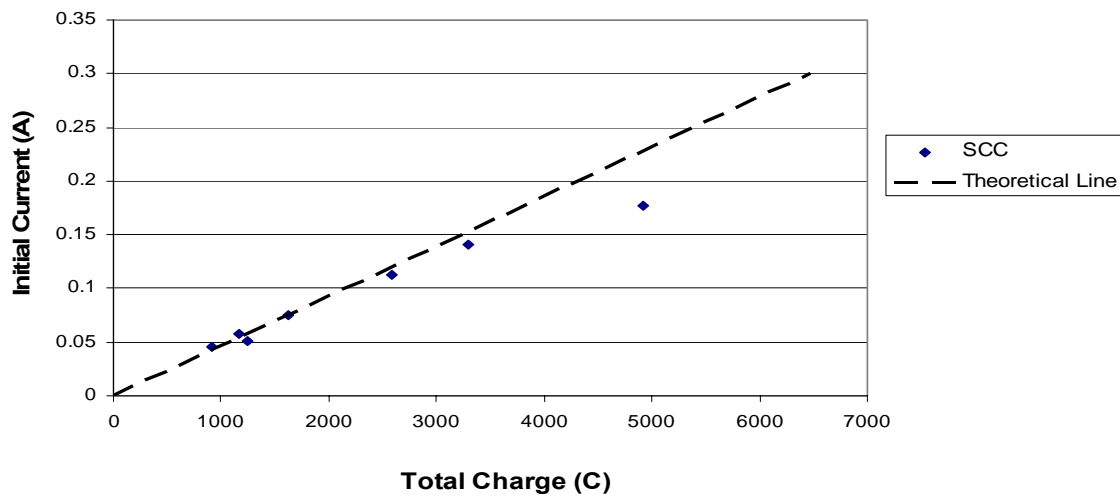


Figure 4.12 Initial current vs total charge

Data points that fall below the theoretical line in Figure 4.6 and 4.12 indicate specimens that experienced higher electrical conductance than would have been predicted using the initial current method. This represents an underestimation of electrical conductance (chloride resistance) from the initial current method. Significant deviations from the theoretical line do not occur until higher charge values and at a charge of 4619 Coulombs there is a deviation of about 22% between the theoretical line and the total charge. Figure 4.13 is a plot of the experimental data in which the charge estimated from the initial current ($Q_{100\text{sec}}$) versus the total charge is shown for the specimens tested at 16 weeks of age. It can be seen that the two methods yield similar results at very low RCPT values, and even at the highest RCPT value the modified method is within 22% of the standard method. As shown in the Table 4.1, the cut-off value for a “high” chloride penetrability concrete is 4000 Coulombs, and therefore the initial current method can be employed instead of the total RCPT charge since significant deviations from the theoretical line do not occur until around the threshold value. Based on these results, only the initial currents were measured for the concrete specimens tested at two weeks of age.

Figure 4.14 shows the total charge (based on the initial current method) for all the specimens. As expected, the age of the concrete specimen is the most significant factor in determining the chloride permeability resistance. However, it is interesting to note that the beneficial effect of fly ash does not occur until a later age and at an early age the permeability is most influenced by the w/b ratio. This is because the pozzolanic reaction proceeds at a slower rate than the cement hydration reaction, but eventually the paste porosity is reduced since the overall solid volume will be increased by the continued pozzolanic reaction. The decrease in porosity increases the durability (decreases the permeability) of the mixes containing fly ash when compared to the mixes without fly ash (S35-F0 and S45-F0). At 16 weeks of age, the chloride permeability of all the mixes with fly ash is significantly lower than those without fly ash; however for a given w/b, there is no significant difference between the chloride permeability for concretes containing 20% fly ash versus 30% fly ash. Comparison of the chloride permeability at 2 weeks versus the chloride permeability at 16 weeks shows that the concretes containing 30% fly ash exhibited a greater reduction in chloride permeability than those containing 20% (Table 4.3)

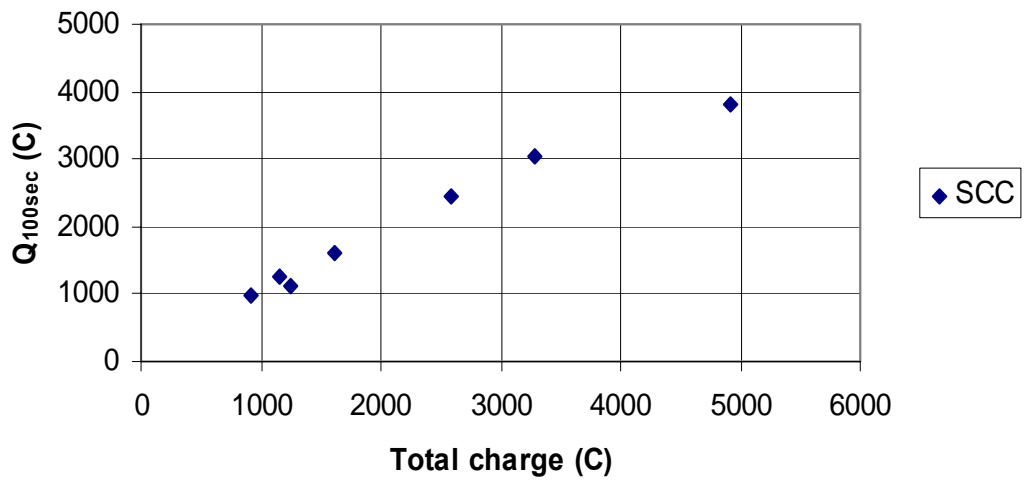


Figure 4.13 Extrapolated total charge vs. actual total charge

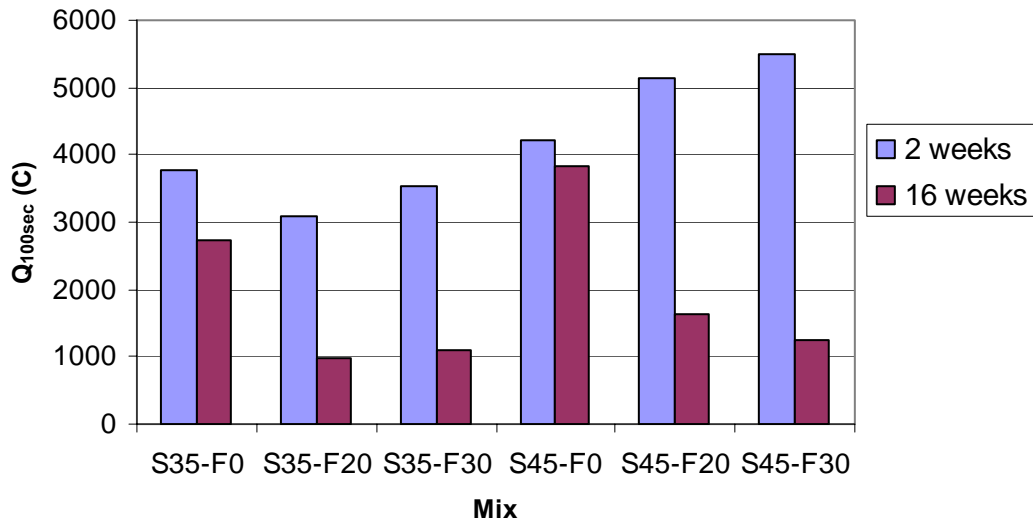


Figure 4.14 RCPT results

Table 4.3 Chloride Penetrability Reduction Percentages

Mix	Q _{100sec} (C)		Reduction (%)
	(2 weeks)	(16 weeks)	
S35-F0	3758	2736	27
S35-F20	3097	983	68
S35-F30	3534	1102	69
S45-F0	4218	3823	9
S45-F20	5141	1624	68
S45-F30	5504	1253	77

4.5 Summary

In this chapter, the hardened state properties were evaluated. Specifically, the compressive strength and chloride penetrability of the hardened concrete created in Chapter 2 were assessed. As expected, addition of fly ash resulted in a reduction of early age strength. The addition of fly ash resulted in a greater strength reduction for the S35 mixes, and this is probably due to the dispersing effect of the superplasticizer.

The permeability of concrete is directly related to its durability. The RCPT method is one test that is often used to assess the chloride penetrability of concrete, and was employed to test the concretes mixes. It was shown that correlation exists between the initial current versus total charge for SCC specimens. At an early age, chloride permeability is most influenced by the water/binder ratio, but the beneficial effect of fly ash in reducing the chloride penetrability occurs at later ages.

Chapter 5 Conclusions

5.1. Introduction

This thesis examines the properties of SCC containing Class F fly ash produced from Illinois region. The fresh state properties of the concrete were assessed using empirical methods such as the slump flow test, L-box test and penetration apparatus test. In addition, the rheology of the paste matrix was evaluated in order to verify a previously developed paste rheology model. Finally, the hardened state properties of compressive strength and permeability were also evaluated. This chapter summarizes the conclusions made in this study and provides suggestions for future work.

5.2. Conclusions

Self-consolidating concrete is still considered by many to be a “special” concrete. Within the last four years, production of SCC in North America has increased and the effort has been largely spearheaded by the precast industry. Understanding the properties of SCC and the ways that local materials affect these properties is important in furthering the usage of SCC. Since SCC is designed with higher paste volumes than normally vibrated concrete, this can lead to a significant increase in cost if the increase in paste volume is gained solely by using more cement. In Illinois over 3 million tons of fly ash is produced annually, and 2.4 millions tons of it is landfilled or ponded. The addition of fly ash as a replacement for cement will not only decrease the price of SCC, but also there are also environmental benefits that occur from the utilization of a waste material and the reduction in landfill space.

In chapter one, the development of SCC was presented and a discussion on mixture proportioning and fly ash was also given. Chapter 2 began with reviewing the key fresh state properties of SCC and discussing common testing methods. The results from this chapter show that it is possible

to produce a good performing SCC using type F fly ash. For similar workability, the addition of fly ash resulted in a decrease in superplasticizer dosage. Chemical admixtures such as superplasticizers are generally an expensive component, and reducing the amount of superplasticizer used in SCC aids in keeping the price of SCC down.

In chapter 3, a review of rheology was given and the paste rheology model was introduced. As expected, for a given w/b, the addition of fly ash decreases the viscosity. This supports previous findings that there are rheological benefits to using fly ash without increasing the superplasticizer dosage or increasing the water demand. The results indicate that paste rheology model does a good job of predicting the fresh state performance of the concrete for mixes, but the mixes used in the model should have density differences between the aggregate and the matrix that are similar to the ones that were used to develop the model. Otherwise, large deviations can occur, and it was apparent that small differences in the density difference could have major effects. This is believed to be due to the effect of the density difference and the confounding that occurs in the flow/viscosity ratio from low viscosities measurements. It was determined that both aggregate spacing (D_{ss}) and the product ($P_{\Delta r}$) between average aggregate radius and difference between densities of aggregates and paste influence the correlation of paste rheology with fresh SCC's properties.

In chapter 4, the compressive strength and chloride permeability of the concrete were evaluated using ASTM C-39 and ASTM C-1202, respectively. The addition of fly ash resulted in reduced compressive strength, however all mixes were able to obtain strengths exceeding 15 MPa after one day. A relationship between superplasticizer/binder dosage and compressive strength was also discussed. For the RCPT test, it was shown that there is a correlation between initial current and total charge for SCC. The results show that at an early age, chloride permeability is most influenced by the water/binder ratio. However, at later ages the beneficial effects of fly ash is apparent and is the governing parameter in reducing permeability.

5.3. Research Extensions

There are a number of areas that could be explored in the evaluation of SCC. Foremost, further investigation should be done on the effect of density difference on the rheological properties of SCC. A better understanding on how the density difference affects the yield stress and viscosity of paste would enable it to be incorporated into the rheological model. This would make the model more generalized and robust. In addition, a study on the rheology of paste and its relationship to the rheology of concrete could provide insight on the mechanism controlling the filling ability, passing ability, and segregation resistance of SCC. Furthermore, an investigation on the pore structure of SCC, other properties that effect durability (air permeability, gas permeability, freeze-thaw resistance, etc) and a study correlating the ponding tests results with RCPT values for SCC may be another avenue to explore. Finally, future work in the area of understanding the role that thixotropy and investing the relationship between T50 and viscosity would provide insight on how rheology influences concrete placement.

References

ASTM C29/C29M-97 Standard Test Method for Bulk Density ("Unit Weight") and Voids in Aggregate. PA: 1-4.

ASTM C1202-97 Standard Test Method for Electrical Indication of Concrete's Ability to Resist Chloride Ion Penetration. PA: 639-643.

Bhatty, J. I. and P. F. G. Banfill (1982). "Sedimentation Behaviour in Cement Pastes Subjected to Continuous Shear in Rotational Viscometers." Cement and Concrete Research **12**: 69-78.

Bonen, D. and S. P. Shah (2004). The Effects of Formulation on the Properties of Self-Consolidating Concrete. Concrete Science and Engineering: A Tribute to Arnon Bentur, North America
Evanston, IL.

Bui, V. K., Y. Akkaya, et al. (2002). "Rheological Model Self-Consolidating Concrete." ACI Materials Journal **99**(6): 549-559.

Bui, V. K., D. Montgomery, et al. (2002). "Rapid Testing Method for Segregation Resistance of Self-Compacting Concrete." Cement and Concrete Research **32**(9): 1489-1496.

EFNARC (2002). Specification and Guidelines for Self-Compacting Concrete.

Ferraris, C. F. (1999). "Measurement of Rheological Properties of High Performance Concrete: State of the Art Report." Journal of Research of the National Institute of Standards and Technology **104**(5): 461-478.

Ferraris, C. F., H. O. Karthik, et al. (2001). "The influence of mineral admixtures on the rheology of cement paste and concrete." Cement and Concrete Research: 245-255.

Geiker, M. R., M. Brandl, et al. (2002). "The effect of measuring procedure on the apparent rheological properties of self-compacting concrete." Cement and Concrete Research: 1791-1795.

Gibbs, J. and W. Shu (1999). Strength of Hardened Self-Compacting Concrete. 1st RILEM Symposium on Self-Compacting Concrete, Stockholm, Sweden, RILEM Publications S.A.R.L.

Ichimiya, K., T. Idemitsu, et al. (2000). Influence of the Fluidity of Mortar and Condition of Form-Concrete Interface on the Characteristics of Surface Voids in Self-Compacting Concrete. Transactions of the Japan Concrete Institute.

Illinois State Geological Survey (2003). Coal Geology of Illinois. Keystone Coal Industry Manual.

Kennedy, C. T. (1940). The Design of Concrete Mixes. Proceedings of the American Concrete Institute.

Khayat, K. H. and H. Monty (1999). Stability of Self-Consolidating Concrete, Advantages, and Potential Applications. 1st RILEM Symposium on Self-Compacting Concrete, Stockholm, Sweden, RILEM Publications S.A.R.L.

Klug, Y. and K. Holschemacher (2003). Comparison of the Hardened Properties of Self-Compacting and Normal Vibrated Concrete. 3rd International Symposium on Self-Compacting Concrete, Reykjavik, Iceland.

Kokado, T. (1999). "Study on a Method of Obtaining Rheological Coefficient of High-Flow Concrete from Slump Flow Test." Journal of Materials, Concrete Structures and Pavement of JSCE: 113-130.

Kosmatka, S. H., B. Kerkhoff, et al. (2002). Design and Control of Concrete Mixtures. Skokie, Portland Cement Association.

Mather, B. and C. Ozyildirim (2002). Concrete Primer. Farmington Hills, American Concrete Institute.

McGrath, P. F. and R. D. Hooton (1999). "Re-evaluation of the AASHTO T259 90-day salt ponding test." Cement and Concrete Research **29**: 1239–1248.

Mindess, S., J. F. Young, et al. (2003). Concrete. Upper Saddle River, Prentice Hall.

Nielsson, I. and O. Wallevik (2003). Rheological Evaluation of Some Empirical Test Methods-Preliminary Results. Third International Symposium on Self Compacting Concrete, Reykjavik, Iceland, RILEM Publications S.A.R.L.

Noguchi, T., S. G. Oh, et al. (1999). Rheological Approach to Passing Ability Between Reinforcing Bars of Self-Compacting Concrete. 1st International Rilem Symposium on Self-Compacting Concrete, Stockholm, Sweden, RILEM Publications S.A.R.L.

Okamura, H. (1997). "Self-Compacting High-Performance Concrete." Concrete International: 50-54.

Okamura, H. and M. Ouchi (1999). Self-Compacting Concrete. Development, Present Use and Future. 1st International RILEM Symposium on Self-Compacting Concrete, Stockholm, Sweden, RILEM Publications S.A.R.L.

Ouchi, M. and Y. Nakajima (2001). A Guide for Manufacturing and Construction of Self-Compacting Concrete -Learning from Real Troubles.

PCI FAST Team (2003). "Interim Guidelines for the Use of Self-Consolidating Concrete in PCI Member Plants." PCI Journal: 14-18.

Raghavan, K. P., B. S. Sarma, et al. (2002). Creep, Shrinkage and Chloride Permeability Properties of Self-Consolidating Concrete. First North America Conference on the and Use of Self-Consolidating Concrete, North America Evanston, IL.

Ramsburg, P. (2003). "The SCC Test: Inverted or Upright?" Concrete Producer.

Saak, A. (2000). Characterization and Modeling of Rheology of Cement Paste: With Applications Toward Self- Flowing Materials. Material Science and Engineering. Evanston, Northwestern University: 249.

Saak, A., H. M. Jennings, et al. (2001). "New Methodology for Designing Self-Compacting Concrete." ACI Materials Journal **98**(6): 429-439.

Sakai, E., S. Hoshimo, et al. (1997). The fluidity of cement paste with various types of inorganic powders. 10th International Congress on the Chemistry of Cement, Sweden.

Shane, J. D., C. M. Aledea, et al. (1999). "Microstructural and pore solution changes induced by the rapid chloride permeability test measured by impedance spectroscopy." Concrete Science and Engineering **1**: 110-119.

Stanish, K. D., R. D. Hooton, et al. Testing the Chloride Penetration Resistance of Concrete: A Literature Review, University of Toronto.

Struble, L. J., U. Puri, et al. (2001). "Concrete Rheometer." Advances in Cement Research **13**(2): 53-63.

Tang, C.-W., T. Yen, et al. (2001). "Optimizing Mixture Proportions for Flowable High-Performance Concrete via Rheology Tests." ACI Materials Journal **98**(6): 493-502.

Tattersall, G. H. (1976). "Relationship Between the British Standard Tests for Workability and the Two-Point Test." Magazine of Concrete Research **28**(96): 143-147.

Tattersall, G. H. and P. F. G. Banfill (1983). The Rheology of Fresh Concrete. Marshfield, Pitman Publishing Inc.

Tragardh, J. (1999). Microstructural Features and Related Properties of Self-Compacting Concrete. 1st RILEM Symposium on Self-Compacting Concrete, Stockholm, Sweden, RILEM Publications S.A.R.L.

U.S. Department of the Interior (2004). Mineral Industry Surveys.

Wallevik, O. H. (2003). Rheology - A Scientific Approach To Develop Self-Compacting Concrete. 3rd International RILEM Symposium, Reykjavik, Iceland, RILEM Publications S.A.R.L.

Wang, K., D. C. Jansen, et al. (1996). "Permeability Study of Cracked Concrete." Cement and Concrete Research **27**(3): 381-394.

Westerholm, M., P. Skoglund, et al. (2002). Chloride Transport and Related Microstructure of Self-Consolidating Concrete. First North American Conference on the Design and Use of Self-Consolidating Concrete, North America Evanston, IL.

Appendix A: Sample Analysis to Determine Viscosity

S35-F0:

shear_stress
shear_stress_upslope
----->
fit(shear_rate_upslope)



shear_rate

$$\text{fit}(100) = 35.923$$

$$\text{fit}(100) = 35.923$$

$$\eta := \frac{\text{fit}(100)}{100}$$

$$\eta = 0.359 \text{ Pa}\cdot\text{s}$$